ACR No. 4A14

NATIONAL ADVISORY COMMITTEE FOR AERONAUTICS

WARTIME REPORT

ORIGINALLY ISSUED
January 1944 as
Advance Confidential Report 4A14

WIND-TUNNEL INVESTIGATION OF AILERONS ON A LOW-DRAG AIRFOIL

I - THE EFFECT OF AILERON PROFILE

By Robert M. Crane and Ralph W. Holtzclaw

Ames Aeronautical Laboratory
Moffett Field, California

NACA

WASHINGTON

NATIONAL ADVISORY COMMITTEE FOR AERONAUTICS

ADVANCE CONFIDENTIAL REPORT

WIND-TUNNEL INVESTIGATION OF AILERONS ON A LOW-DRAG AIRFOIL

I - THE EFFECT OF AILERON PROFILE

By Robert M. Crane and Ralph W. Holtzclaw

SUMMARY

An investigation was made in the Ames Aeronautical Laboratory 7- by 10-foot wind tunnel of the effects of various modifications to the profile of a 0.20-chord plain sealed aileron and a 0.15-chord plain sealed aileron on an NACA 66,2-216 (a = 0.6) airfoil. Aileron profiles tested consisted of one profile conforming to the normal NACA 66,2-216 (a = 0.6) ordinates; a profile consisting of straight-line surfaces from the trailing edge to the hinge-line ordinates; an intermediate thickened profile; and a profile thinned below the normal airfoil ordinates.

Thickening of the aileron profile was found to reduce the aileron effectiveness, reduce the slope of the wing section lift curve, and reduce the hinge-moment coefficients. Thinning the profile had the opposite effect. The effects of profile on the aileron characteristics decreased with increasing angle of attack, there being practically no effect at an angle of attack of 12°. Thickening the profile caused a slight increase in minimum profile-drag coefficient, but thinning the profile had no effect.

It is demonstrated that deviations of the order of $\pm 0.005c_a$ from the specified profile on the ailerons of a typical pursuit airplane can cause stick-force variations of ±20 pounds for a large rate of roll at an indicated airspeed of 300 miles per hour. It is also shown that the danger of overbalance at small deflections of closely balanced ailerons can be diminished by thickening of the aileron profile if the internal-balance chord is simultaneously reduced to maintain the same stick force for a large rate of roll.

INTRODUCTION

With every increase in size and speed of modern high-performance airplanes, the problem of attaining adequate lateral control without excessive control forces becomes less amenable to solution by simple aerodynamic balancing methods. Of the various methods of aerodynamic balance available, one of the most efficient is the sealed internal nose balance. However, sufficient control lightness frequently cannot be satisfactorily attained by the use of an internal nose balance alone. The necessary balance may be so large that the required control-surface deflection cannot be attained, or structural necessities of the main surfaces may be such that adequate balance cannot be incorporated in the design. Aileron profile offers an independent means of adjusting aileron hinge moments without the additional linkages and loss in effectiveness associated with a balancing tab. Aileron profile also offers a convenient means of adjusting the aileron control characteristics of an existing installation without the structural modifications required by changes of aileron plan form or aerodynamic nose balance. The efficacy of profile variations in modifying aerodynamic characteristics, and the consequent necessity of fabricating to close tolerances, must be appreciated when it is desired to obtain specified aileron characteristics on any one airplane or to maintain a reasonable constancy of characteristics in a number of airplanes of the same design.

The purpose of the tests reported herein was to provide quantitative data on the effect of aileron profile variations and to form a logical basis for the specification of aileron tolerances.

MODEL AND APPARATUS

Model

The airfoil used in these tests was constructed of laminated mahogany to the NACA 66,2-216 (a = 0.6) profile of 4-foot chord and 5-foot span. The airfoil ordinates are given in table I. The aft 0.35 chord of the airfoil was made removable to allow the testing of ailerons of various chords. A soli trailing-edge section was constructed and this section and the main airfoil were equipped with a single row of pressure orifices built into the upper and lower surfaces of the airfoil at the midspan section. These orifices were located on the model as listed in table II. The ailerons were constructed of laminated mahogany and had a nose-gap seal of dental rubber dam. The aileron ordinates are given in table III. The ordinates of the normal-profile aileron are the same as the corresponding ordinates of the NACA 66,2-216 (a = 0.6) airfoil. The details of the ailerons, and the modifications tested, are shown in figures 1 and 2.

TEST INSTALLATION

The airfoil was mounted vertically in the test section of the 7- by 10-foot wind tunnel No. 1, as shown in the photographs of figure 3. End plates were fastened to the 5-foot-span section. Fairings of the same airfoil section as the wing were attached to the tunnel-floor and ceiling turntables and were used to shield the connection between the model and the balance frame. These fairings were not equipped with ailerons. Provisions were made for changing the angle of attack and the aileron angle while the tunnel was in operation. Aileron hinge moments were measured by means of electrical resistance-type strain gages which were mounted on a member which restrained the torque tube of the aileron from rotation.

COEFFICIENTS AND CORRECTIONS

The coefficients used in the presentation of results follow.

c_n airfoil section normal-force coefficients (n/qc)

c_l airfoil section lift coefficient (l/qc)

c_{d_o} airfoil section profile-drag coefficient (d_o/qc)

c_m airfoil section pitching-moment coefficient (m/qc^2)

c_h aileron section hinge-moment coefficient $(h/qc_a{}^2)$

P/q internal static pressure at aileron nose divided by dynamic pressure (See fig. 1.)

Δc_l increment of c_l due to deflecting the aileron from neutral

$\Delta c_l{}'$ c_l of down aileron minus c_l of up aileron

Δc_{d_o} increment of c_{d_o} due to dflecting the aileron from neutral

Δc_h increment of c_h due to deflecting the aileron from neutral

$\Delta c_h{}'$ c_h of up aileron minus c_h of down aileron

$\Delta P/q$ increment of pressure coefficient across aileron nose seal (pressure below seal minus pressure above seal divided by dynamic pressure)

where

n airfoil section normal force

l airfoil section lift

d_o airfoil section profile drag

m airfoil section pitching moment about quarter-chord of airfoil

h aileron section hinge moment

c chord of airfoil with aileron neutral

c_a chord of aileron aft of aileron hinge line

q dynamic pressure of air stream $(1/2\rho V^2)$

V free-stream velocity

In addition to the above, the following symbols are employed:

α_o angle of attack for airfoil of infinite aspect ratio

δ_a aileron deflection with respect to the airfoil

d increment above the normal profile of the upper and lower surface ordinates of the modified aileron profiles at $0.5c_a$

b wing span of assumed airplane

V_i indicated airspeed, miles per hour

p rate of roll, radians per second

$c_{l_\alpha} = (\partial c_l/\partial \alpha)_{\delta_a=0}$ (measured through $\alpha_o = 0^\circ$)

$c_{l_{\delta_a}} = (\partial c_l/\partial \delta_a)_{\alpha_o=0}$ (measured through $\delta_a = 0^\circ$)

$c_{h_\alpha} = (\partial c_h/\partial \alpha)_{\delta_a=0}$ (measured through $\alpha_o = 0^\circ$)

$c_{h_{\delta_a}} = (\partial c_h/\partial \delta_a)_{\alpha_o=0}$ (measured through $\delta_a = 0^\circ$)

The subscripts outside the parentheses represent the factors held constant during the measurement of the parameters.

The lift coefficient, profile-drag coefficient, and pitching-moment coefficient have been corrected for tunnel-wall effects. Section profile drag was determined by measurement of loss of momentum in the wing wake. A comparison of force-test and pressure-distribution measurements of section lift coefficient and section pitching-moment coefficient indicated that the end plates had no effect on these coefficients with aileron neutral. No corrections have been applied to section hinge-moment coefficients and no end-plate correction has been applied to Δc_l. Because of possible tip losses, it is believed that the measured aileron effectiveness is slightly low and rates of roll computed from these data will be conservative. By comparison of these data with section data on a similar airfoil (reference 1), it is estimated that the maximum decrease in measured Δc_l due to this effect is not more than 12 percent.

TESTS

For each of the aileron-profile modifications, two series of tests were made. The first series obtained aileron characteristics at the highest Reynolds number obtainable (9,000,000) at five angles of attack (-4°, -2°, 0°, 2°, and 4°). A second series at angles of attack of 0°, 4°, 8°, and 12° was run at a reduced Reynolds number

(3,800,000). With the aileron neutral, section characteristics were obtained at a Reynolds number of 8,200,000. Section profile-drag coefficients were obtained with the aileron neutral, at the ideal lift coefficient ($c_l = 0.21$) over a Reynolds number range of 3,000,000 to 10,000,000.

RESULTS AND DISCUSSION

Basic section data.- The basic section data, with aileron deflected and aileron neutral, are presented in figures 4 to 14. These data may be utilized to predict the section characteristics of ailerons with any amount of internal nose balance by means of the equation

$$(c_h)_B = c_h + \Delta P/q \ \frac{B^2 - R^2}{2}$$

where

$(c_h)_B$ aileron section hinge-moment coefficient of aileron with sealed internal nose balance

c_h aileron section hinge-moment coefficient of plain aileron

B nose balance (expressed as fraction of c_a)

R nose radius of plain aileron (expressed as fraction of c_a)

While these basic data are useful for purposes of aileron design, the prediction and comparison of the effects of aileron profile on section characteristics may be more conveniently demonstrated by means of section parameters. For this purpose plots showing the relation of various coefficients and parameters to other independent variables have been prepared.

Aileron effectiveness.- The effect of the profile variations on the aileron-effectiveness parameter $(\partial\alpha/\partial\delta_a)_{c_n}$ and $c_{l_{\delta_a}}$ is shown in figures 16 to 18. It will be noted that the value of the former quantity for the normal-profile aileron, at a Reynolds number of 9,000,000, is about 71 percent of that which would be predicted from thin-airfoil theory, and about 90 percent of the value obtained on the NACA 0009 airfoil (reference 2). Thickening the aileron profile reduces the aileron effectiveness, and thinning the profile increases it. The change in the effectiveness is very close to a linear function of d (figs. 17 and 18).

Aileron profile has a similar influence on effectiveness at the higher aileron deflections where the flow over the aileron has separated. Figures 19 and 20 present the total $\Delta c_l'$ available due to $\pm 10^\circ$ and $\pm 15^\circ$ of aileron deflection plotted against angle of attack. At moderate angles of attack thickened profiles give the lower effectiveness values; thinned profiles give the higher. However, differences due to profile decrease at the higher angles of attack and at an α_o of 12° there is only a minor variation in $\Delta c_l'$ available for the various aileron profiles. The $\Delta c_l'$ available under these extreme conditions of angle of attack and aileron deflections is about 41 percent of the $\Delta c_l'$ predicted on the assumption of thin-airfoil effectiveness (that is, by using the $\partial\alpha/\partial\delta_a$ relationship from reference 3 and using a value of c_{l_α} of $2\pi/57.3$). This value holds within 2 percent for both the 0.15-chord ailerons and the 0.20-chord ailerons and for all the profile variations.

To determine the effect of control-surface profile on the aileron effectiveness of a typical installation, these data have been applied to the prediction of the aileron control characteristics of a modern pursuit airplane. The airplane data necessary for the calculations are presented in table IV. The calculations have been made assuming zero sideslip of the airplane and no torsional deflection of the wing. The effect of aileron profile on c_{l_α} has been included in determination of C_{l_p}, the damping-moment coefficient due to rolling. The calculation variation of $pb/2V$ with total aileron deflection for the various aileron profiles is presented in figures 21 and 22 for indicated airspeeds of 300 and 120 miles per hour. Examination of these figures reveals that the aileron effectiveness at low speeds is little influenced by aileron profile. Thus, the size and the total deflection for an installation of given effectiveness will be unchanged by control-surface profile modifications.

Aileron hinge moments.- The variation of $c_{h_{\delta_a}}$ with control-surface chord is shown in figure 23, and a comparison is afforded with the variation predicted from thin-airfoil theory and that measured on an NACA 0009 airfoil (reference 2). The value of $c_{h_{\delta_a}}$ for the normal-profile aileron, at a Reynolds number of 9,000,000, is about 58 percent of the value predicted by thin-airfoil theory and about 82 percent of the measured value for the NACA 0009 airfoil.

The aileron hinge-moment parameters c_{h_α} and $c_{h_{\delta_a}}$ are plotted in figures 17 and 18 as functions of d. The curves indicate that both of these parameters vary approximately linearly with d, increasing algebraically as d is increased. A similar relationship has been established by reference 4. The value of $(\partial c_h/\partial \alpha)_{\delta_a}$ varies with angle of attack and aileron deflection. At small angles of attack and zero aileron deflection, there is a linear relationship between $(\partial c_h/\partial \alpha)_{\delta_a=0}$ and d. The value of $(\partial c_h/\partial \alpha)_{\delta_a=0}$ in this region varies between -0.0087 for $d = -0.01c_a$ and 0.0024 for $d = 0.02c_a$. At angles of attack greater than 6°, $(\partial c_h/\partial \alpha)_{\delta_a=0}$ has an approximately constant value of -0.010 irrespective of aileron profile. At low angles of attack and extreme aileron deflections, the effect of aileron profile on $(\partial c_h/\partial \alpha)_{\delta_a}$ becomes less less apparent. Data obtained with the straight-sided aileron at low angles of attack (fig. 8) indicate that at zero aileron deflection $(\partial c_h/\partial \alpha)_{\delta_a}$ is positive, at aileron deflections of -12° and 6° the value of $(\partial c_h/\partial \alpha)_{\delta_a}$ is zero, and at larger aileron deflections its value becomes negative.

The variation of total $\Delta c_h{}'$ due to $\pm 15^\circ$ of aileron deflection with angle of attack is presented in figures 24 and 25. The value of $\Delta c_h{}'$ decreases as d is increased, but at large angles of attack the effect of profile is very small.

The data of figures 17 and 18 have been plotted in figures 26 and 27 as hinge-moment parameters against lift parameters. These curves show the relative dependence of the aileron hinge moments on the aileron effectiveness and on the slope of the wing section lift curves. In addition to the data shown for the ailerons of the present investigation, experimental points are included from data obtained for a series of 0.20-chord ailerons with thickened and beveled trailing edges. The small deviation of the experimental points from the mean curves indicates that the relationships indicated are not influenced by the chordwise distribution of thickness of the control-surface profile. An experimental point is also presented from data obtained on an NACA 0009 airfoil (reference 2) which indicates that for the same effectiveness, similar hinge moments may be anticipated for ailerons on an NACA 66,2-216 (a = 0.6) airfoil as are experienced on ailerons on an NACA 0009 airfoil. A similar agreement between the subject data and the NACA 0009 data does not exist for c_{h_α} against c_{l_α}.

Since the effect of aileron profile on $\Delta P/q$ is small, the hinge-moment coefficients of ailerons with internal nose balance will exhibit aileron profile effects similar to those observed on the plain ailerons. As separation occurs over the aileron at large deflections, there is an abrupt loss in P/q over the suction side of the control (side opposite the deflection). This loss accounts for the nonlinearity of the curves of $\Delta P/q$ against δ_a (figs. 5 to 12). It is this reduction in $\Delta P/q$ which causes the nonlinearity of hinge-moment curves of ailerons with large amounts of internal nose balance.

Figures 28 and 29 illustrate the changes in control-force characteristics which result from small changes in aileron profile. The variation of stick force with $pb/2V$ for a typical modern pursuit airplane equipped with 0.20-chord ailerons with $0.534c_a$ internal nose balance is presented in these figures for indicated airspeeds of 300 and 120 miles per hour. At the higher speed, a decrease of $0.009c_a$ in the aileron ordinates at $0.5c_a$ reduces the $pb/2V$ obtainable with a 30-pound stick force from 0.08 to 0.056 and more than doubles the stick force for a $pb/2V$ of 0.08. Increasing the midchord ordinates of the aileron $0.0009c_a$ changes the stick force from 8 pounds to an overbalance of 7 pounds at a $pb/2V$ of 0.05. Since results of overbalance are likely to prove catastrophic in a high-speed dive, due to the ailerons taking control, every effort should be made to maintain manufacturing tolerances and allowable surface deformations at a value which would preclude the occurrence of this condition.

The possible use of aileron profile changes to obtain desired stick-force characteristics is illustrated by figures 30 and 31. Control-force characteristics are shown for a typical modern pursuit airplane equipped with 0.20-chord ailerons. The airplane data necessary for the calculations are presented in table IV. Each aileron was assumed to have an internal nose balance such that a $pb/2V$ of 0.08 can be obtained with a 30-pound stick force at an indicated airspeed of 300 miles per hour. It will be observed that the thin-profile aileron which is closely enough balanced to satisfy the 30-pound stick-force limitation at high speed is overbalanced 4 pounds at a $pb/2V$ of 0.035. As the aileron profile is thickened, the control-force gradient becomes more positive, and the linear range of the gradient is extended to larger values of $pb/2V$. The primary problem of aileron-balance design is to make the control light enough at very high speed while avoiding overbalance in any part of the deflection range, and retaining sufficient feel at low speeds. The danger of overbalance can be minimized by the attainment of a linear variation of control force with $pb/2V$ at high speeds. The nonlinearity of the hinge-moment curves of ailerons designed with internal nose balance prevents the realization of this ideal condition, but aileron profile offers a limited means of controlling the value and the linear range of this control-force gradient. These effects of aileron profile on control-force gradients are due mainly to two causes: the reduction in the amount of nose balance required by the thickened aileron profiles, with the consequent reduction in the nonlinearity of the hinge-moment curves of the balanced ailerons; and the presence of an unfavorable response characteristic (positive $(\partial c_h/\partial \alpha)_{\delta_a}$) at low aileron deflections (where an increase in stick force is desired), with favorable response at high aileron deflections (where a decrease in stick force is desired). This effect of response on control-force gradient is illustrated by figure 32, presenting the variation of $\Delta c_h'$ and $\Delta c_l'$ for the static condition and for the dynamic rolling condition of the assumed pursuit airplane.

The effect of aileron chord on the control-force characteristics can be obtained by a comparison of the control-force characteristics of the 0.20-chord and 0.15-chord ailerons of normal and straight-sided profile. In all cases where the two ailerons are designed for the same high-speed stick force at a $pb/2V$ of 0.08, the 0.20-chord ailerons produce a more nearly linear variation of stick force with $pb/2V$ than can be acquired with the 0.15-chord aileron. Figure 33 presents the variation of stick force with $pb/2V$ when the ailerons are designed for a 30-pound stick force for a $pb/2V$ of 0.08 on a typical pursuit airplane at an indicated airspeed of 300 miles per hour. The reduction in control-surface chord results in a 20-pound decrease in the stick force for an aileron of normal profile and a 5-pound decrease in the stick force for an aileron of straight-sided profile for a $pb/2V$ of 0.05.

Lift.- The variation of c_{l_α} with d is shown in figures 17 and 18. These curves indicate that c_{l_α} varies approximately linearly with d, decreasing as d is increased.

Pitching moment.- Thickening the aileron profile caused an increase in $(\partial c_m/\partial c_l)_{\delta_a=0}$ corresponding to a forward shift of the aerodynamic center. This is shown in figures 13 and 14.

Drag.- Figure 15 presents the variation of section profile-drag coefficient with Reynolds number at the ideal section lift coefficient ($c_l = 0.21$). Thinning the aileron profile had no effect on the section profile-drag coefficient, but thickening the profile to straight-sided caused an increase in c_{d_0} of 0.0004 for the 0.20-chord aileron and 0.0002 for the 0.15-chord aileron.

Reynolds number.- A Reynolds number effect was found to exist at low angles of attack and further investigation was made over the available Reynolds number range (3,200,000 to 9,000,000). Figures 34 to 36 present $\Delta c_l'$, $\Delta c_h'$, and $\Delta P/q$ against Reynolds number. At small angles of attack, increasing Reynolds number results in a loss in $\Delta c_l'$, $\Delta c_h'$, and $\Delta P/q$. The magnitude of these effects of increasing Reynolds number is a function of d, increasing as d is increased. (See figs. 17 and 18.) At angles of attack beyond the low-drag range (greater than 2° and less than -1°), the Reynolds number effect was considerably reduced. Measurement of the airfoil boundary-layer profiles indicated that these Reynolds number effects were caused by a forward movement of the transition point, with the aileron deflected, due to increasing Reynolds number. This forward movement of transition, resulting in a thickening of the boundary layer at the beginning of the pressure recovery, reduces the peak of the basic incremental lift and results in a less complete recovery, thus causing a decrease in effectiveness and $\Delta P/q$.

CONCLUSIONS

Results of the tests of aileron-profile variations to 0.20-chord plain sealed-gap ailerons and 0.15-chord plain sealed-gap ailerons on the NACA 66,2-216 (a = 0.6) airfoil indicate the following conclusions:

1. Thickening of the aileron profile results in a decrease in the aileron effectiveness, a decrease in the slope of the wing section lift curve, and a decrease in the aileron hinge-moment coefficients. Thinning the profile has the opposite effect. The magnitude of the increment or the decrement is proportional to and varies approximately linearly with the magnitude of the profile alteration.

2. The effects of aileron profile are reduced as angle of attack is increased. At an angle of attack of 12°, aileron profile has no effect on the aileron characteristics.

3. A linear relationship exists between the aileron hinge moments and the aileron effectiveness. Any reduction in hinge moments by profile alteration is accompanied by a corresponding decrease in effectiveness.

4. Thickening the aileron profile causes an increase of 0.0004 in the minimum section profile-drag coefficient. Thinning the profile has no effect on minimum drag.

5. When the ailerons of a typical pursuit airplane are designed for a given control force for a large rate of roll at high speed, the ailerons with thickened profiles have a greater stick force for full deflection at low speeds than the normal or thinned profiles. Thickening the aileron profile results in a more nearly linear variation of stick force with rate of roll at high speeds, provided the internal-balance chord is decreased to maintain the same maximum stick force.

6. When designed for the same high-speed stick force

for a large rate of roll, ailerons of 0.20 chord are preferable to ailerons of 0.15 chord of the same span. Because of the greater effectiveness of the larger chord ailerons, a more nearly linear variation of stick force with rate of roll at high speed can be attained than is possible with the 0.15-chord ailerons.

Ames Aeronautical Laboratory,
National Advisory Committee for Aeronautics,
Moffett Field, Calif.

REFERENCES

1. Denaci, H. G., and Bird, J. D.: Wind-Tunnel Tests of Ailerons at Various Speeds. II - Ailerons of 0.20 Airfoil Chord and True Contour with 0.60 Aileron-Chord Sealed Internal Balance on the NACA 66,2-216 Airfoil. NACA ACR No. 3F18, June 1943.

2. Ames, Milton B., Jr., and Sears, Richard I.: Determination of Control-Surface Characteristics from NACA Plain-Flap and Tab Data. Rep. No. 721, NACA, 1941.

3. Glauert, H.: Theoretical Relationships for an Aerofoil with Hinged Flap. R. & M. No. 1095, British A.R.C., April 1927.

4. Batson, A. S., Preston, J. H., and Warsap, J. H.: Effect on Hinge Moment of Modifying the Section of a Control and in Each Case of Fitting Trailing Edge Strips and a Shrouded Balance. British A.R.C. 5062, S. and C. 1224, May 9, 1941.

5. Wenzinger, Carl J.: Wind-Tunnel Investigation of Ordinary and Split Flaps on Airfoils of Different Profiles. Rep. No. 554, NACA, 1936.

TABLE I.– NACA 66,2-216 (a = 0.6) AIRFOIL

[Stations and ordinates are given in percent of the airfoil chord]

Upper surface		Lower surface	
Station	Ordinate	Station	Ordinate
0	0	0	0
.371	1.242	.629	-1.112
.607	1.501	.893	-1.319
1.091	1.886	1.409	-1.608
2.317	2.615	2.683	-2.127
4.794	3.701	5.206	-2.869
7.284	4.563	7.716	-3.441
9.781	5.308	10.219	-3.934
14.788	6.500	15.212	-4.702
19.806	7.428	20.194	-5.290
24.832	8.155	25.168	-5.741
29.862	8.708	30.138	-6.080
34.897	9.098	35.103	-6.312
39.936	9.356	40.064	-6.462
44.978	9.471	45.022	-6.523
50.023	9.431	49.977	-6.483
55.073	9.224	54.927	-6.336
60.141	8.800	59.859	-6.043
65.191	8.084	64.809	-5.574
70.198	7.068	69.802	-4.866
75.181	5.889	74.819	-4.037
80.148	4.585	79.852	-3.107
85.106	3.265	84.894	-2.177
90.061	1.937	89.939	-1.235
95.021	0.762	94.979	-.432
100	0	100	0
Leading-edge radius: 1.575 Trailing-edge radius: 0.0625			

TABLE II.- ORIFICE LOCATIONS ON NACA 66,2-216 AIRFOIL

[Orifice locations on upper and lower surface of airfoil in percent of airfoil chord from leading edge]

Orifice	Location	Orifice	Location
0	0	13	45
1	.625	14	50
2	1.250	15	55
3	2.500	16	60
4	5	17	65
5	7.500	18	70
6	10	19	75
7	15	20	80
8	20	21	85
9	25	22	90
10	30	23	95
11	35	24	98
12	40		

TABLE III.– AILERON ORDINATES

[Stations given are wing stations and ordinates are in percent of the airfoil chord]

0.20c Ailerons (T. E. radius: 0.0625)								
	Normal profile		Straight-sided profile		Intermediate thickened profile		Thinned profile	
Station	Upper	Lower	Upper	Lower	Upper	Lower	Upper	Lower
81.25	4.27	−2.85	4.27	−2.85	4.27	−2.85	4.27	−2.85
83.33	3.77	−2.45	3.80	−2.55	3.78	−2.50	3.73	−2.40
85.42	3.21	−2.07	3.33	−2.24	3.27	−2.16	3.15	−1.99
87.50	2.65	−1.67	2.88	−1.93	2.76	−1.80	2.53	−1.54
89.58	2.08	−1.28	2.40	−1.61	2.24	−1.45	1.93	−1.11
91.67	1.54	−.91	1.93	−1.30	1.73	−1.11	1.35	−.72
93.75	1.06	−.58	1.44	−.99	1.25	−.79	.88	−.38
95.83	.63	−.33	.98	−.68	.80	−.50	.50	−.16
97.92	.31	−.17	.51	−.36	.41	−.26	.24	−.07
100	0	0	0	0	0	0	0	0
0.15c Ailerons (T. E. radius: 0.0625)								
87.50	2.65	−1.67	2.71	−1.75	2.68	−1.71	2.61	−1.60
89.58	2.08	−1.28	2.26	−1.48	2.17	−1.38	2.00	−1.17
91.67	1.54	−.92	1.82	−1.19	1.69	−1.06	1.39	−.76
93.75	1.06	−.58	1.38	−.90	1.22	−.75	.85	−.38
95.83	.63	−.33	.92	−.60	.78	−.47	.45	−.16
97.92	.31	−.17	.48	−.33	.40	−.25	.21	−.07
100	0	0	0	0	0	0	0	0

TABLE IV.- CHARACTERISTICS OF TYPICAL PURSUIT AIRPLANE

Wing	
Area, square feet	275
Span, feet	41.5
Aspect ratio	6.23
Taper ratio	3:1
Section	NACA 66,2-216 (a = 0.6)
Ailerons	
Span	from 0.5 semispan to tip
Chord	0.20c
Deflection	$\pm 15^{\circ}$
Airplane	
Wing loading, pounds per square foot	33.7
Aileron differential	1:1
Stick travel, inches	± 8

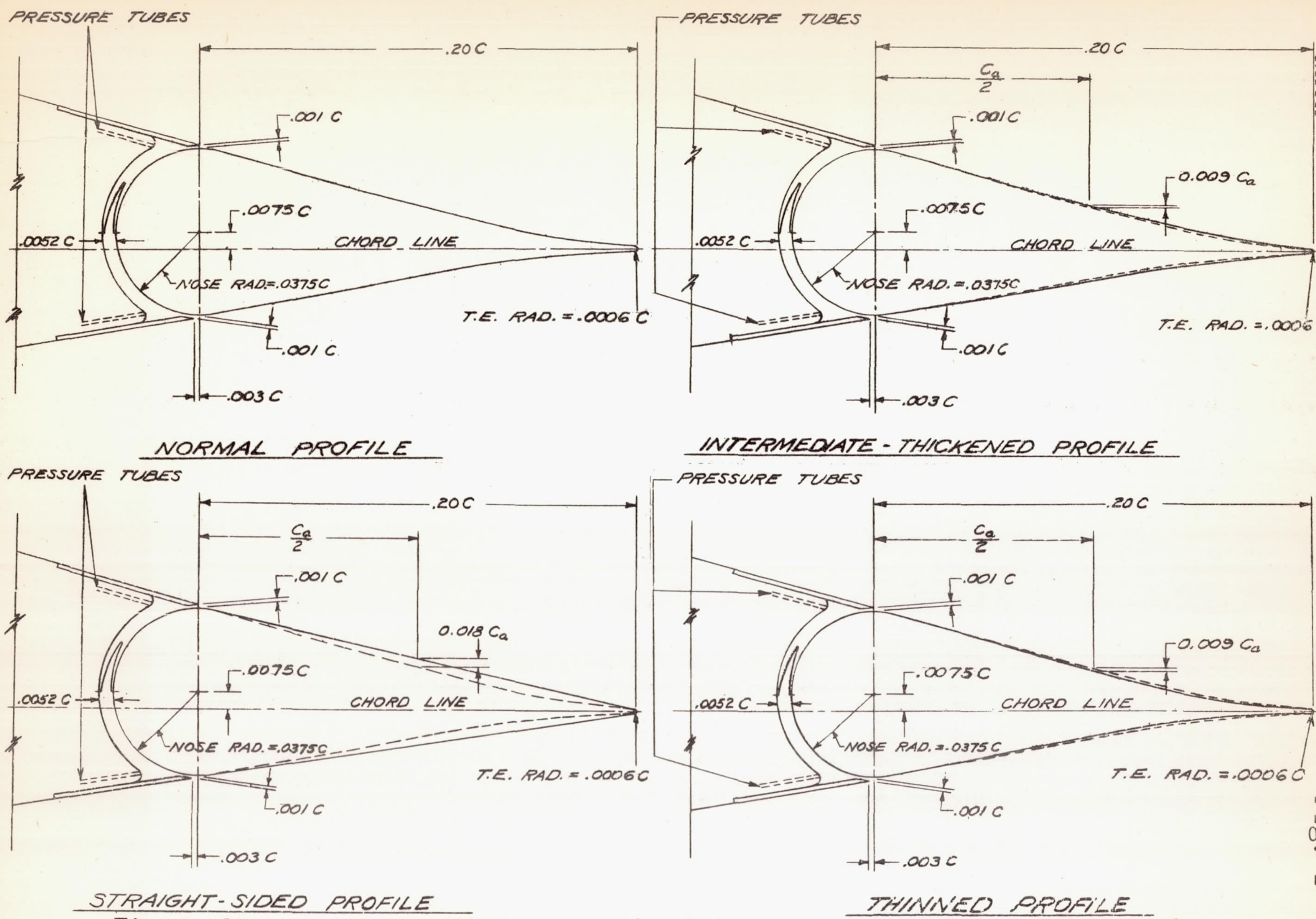

Figure 1.- Profile variations on the 0.20-Chord, Sealed Gap, Plain Aileron.

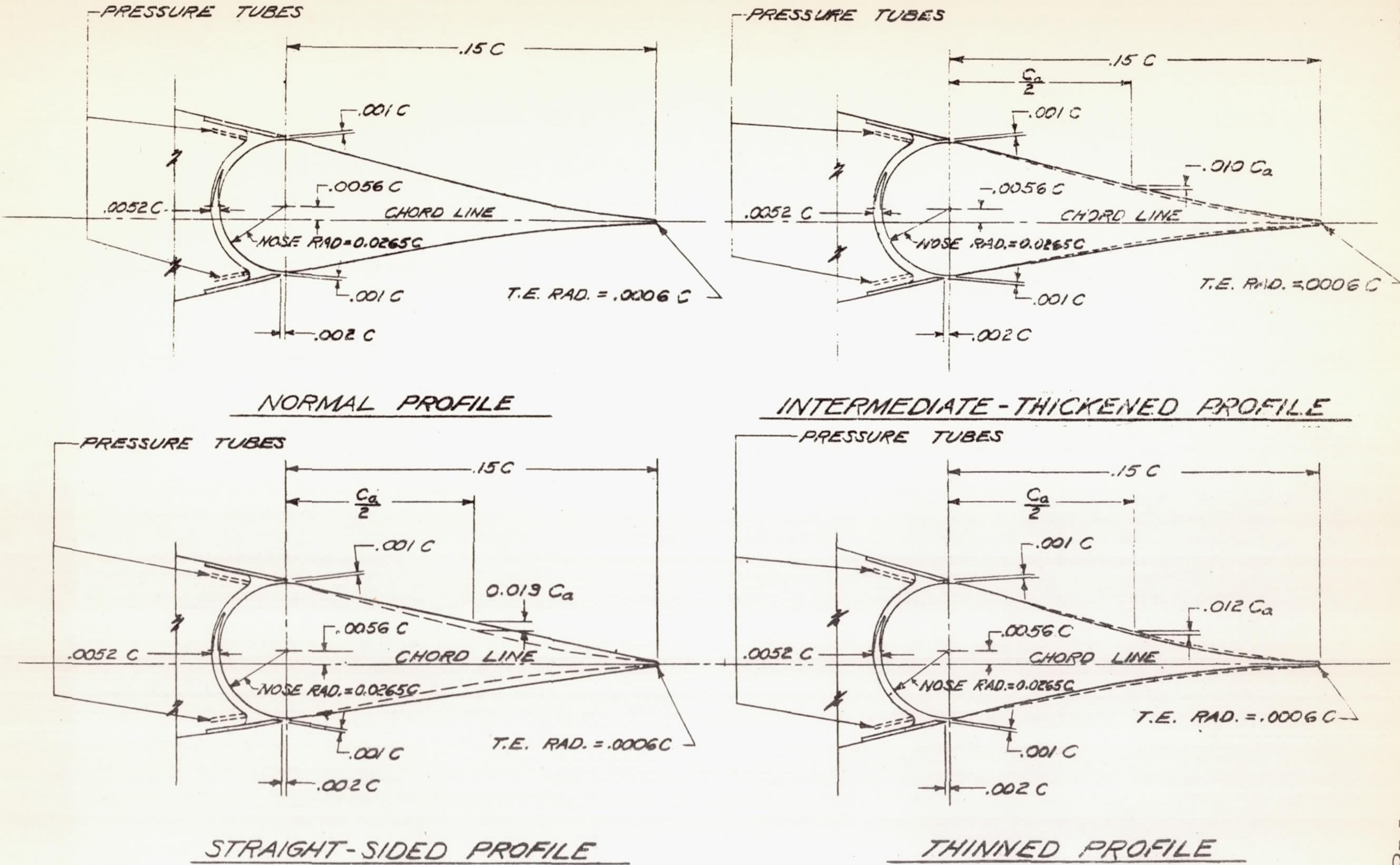

Figure 2.- Profile variations on the 0.15-Chord, Sealed Gap, Plain Aileron.

A-55

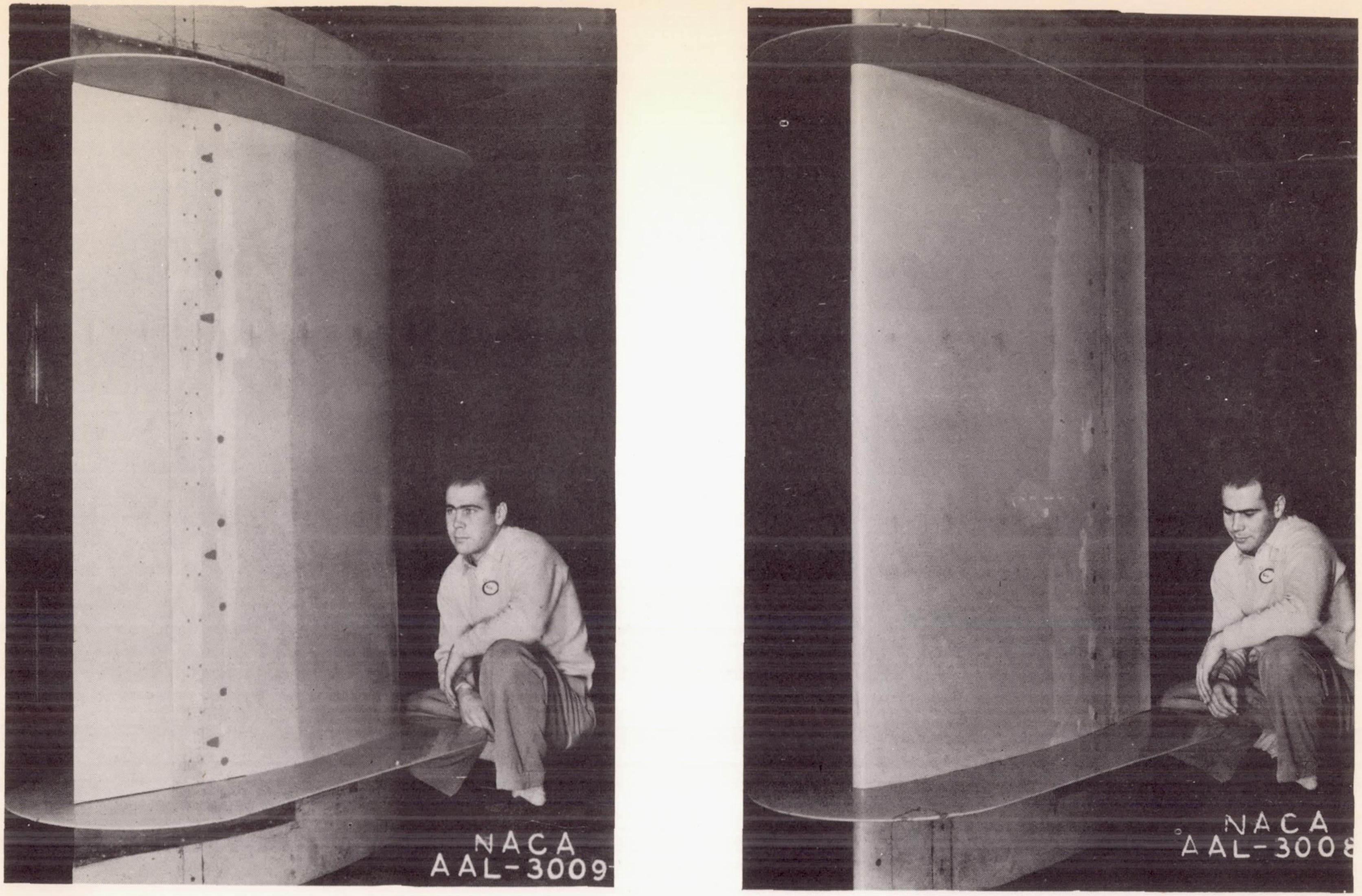

Figure 3.- The NACA 66,2-216 (a = 0.6) airfoil equipped with the 0.20-chord plain aileron of normal profile.

(1 block = 10 divisions on 1/30 Engr. scale)

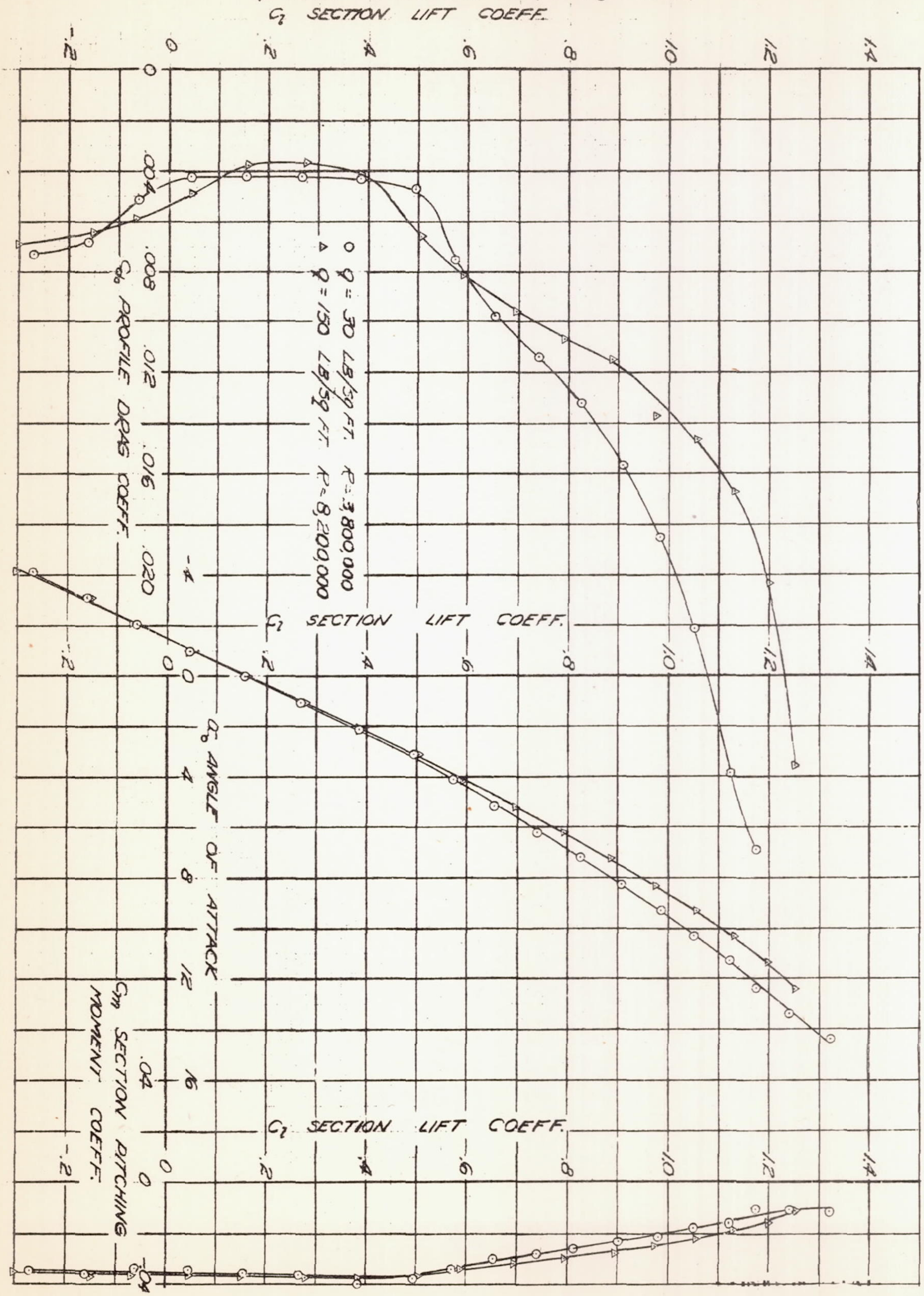

FIGURE 4.- SECTION AERODYNAMIC CHARACTERISTICS OF AN NACA 66,2-216 (a=0.6) AIRFOIL.

A-55

(1 block = 10 divisions on 1/40 Engr. scale)

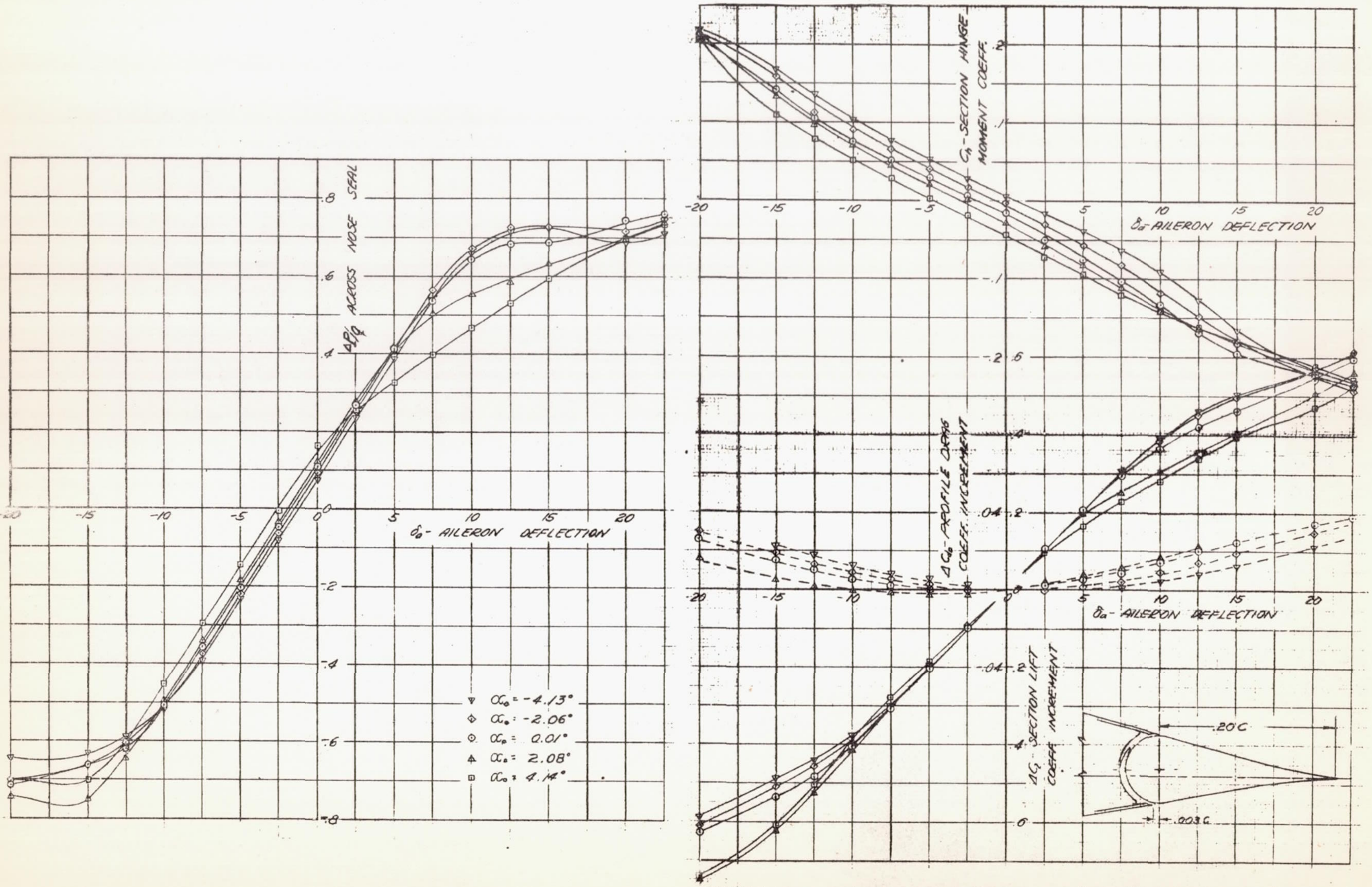

FIGURE 5a.- SECTION AERODYNAMIC CHARACTERISTICS OF AN NACA 66, 2-216 (a = 0.6) AIRFOIL EQUIPPED WITH A 0.20-CHORD, SEALED GAP, PLAIN AILERON OF NORMAL PROFILE.
q = 180 lb /sq ft. R = 3,000,000

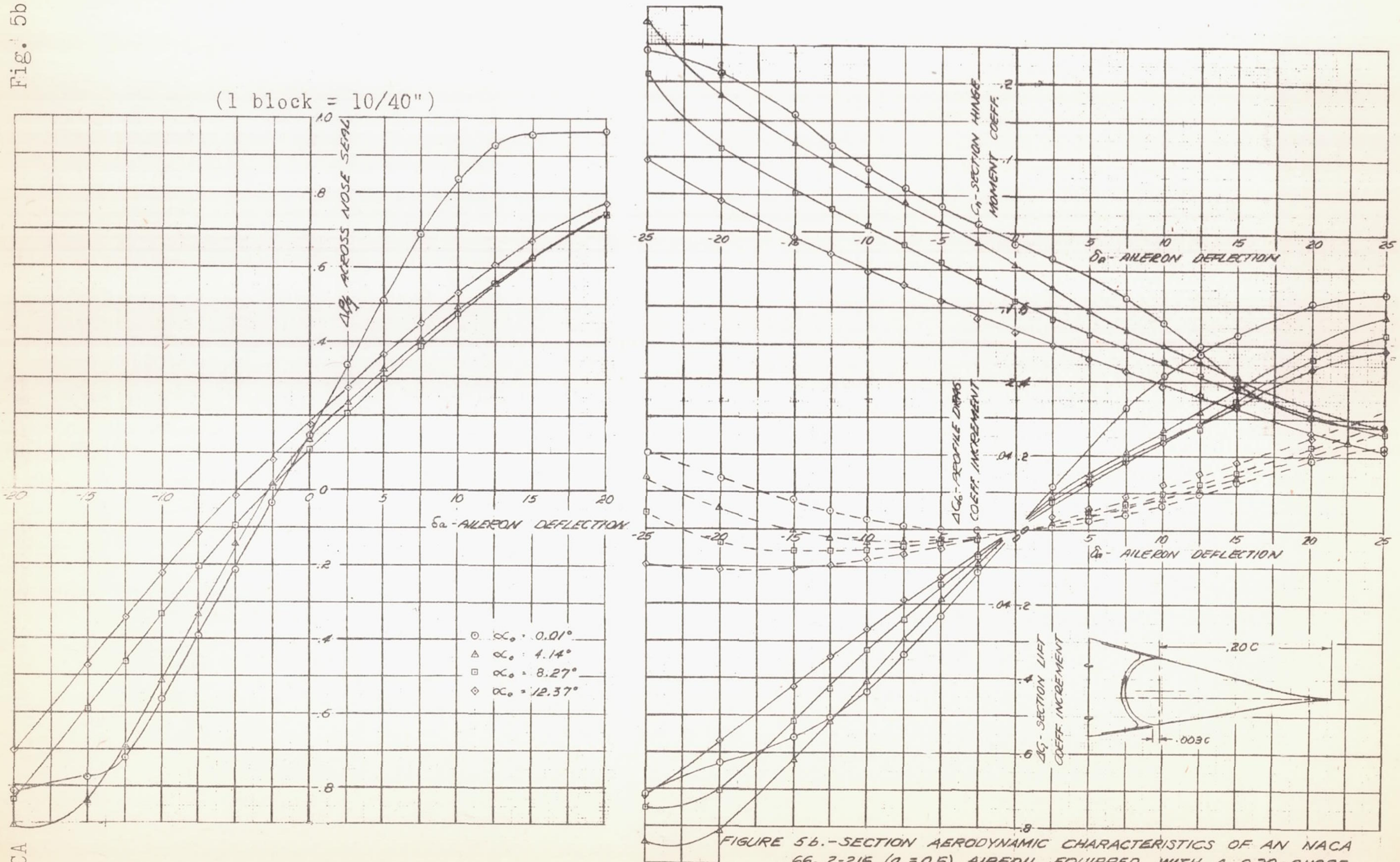

FIGURE 5b.-SECTION AERODYNAMIC CHARACTERISTICS OF AN NACA 66, 2-216 (a = 0.6) AIRFOIL EQUIPPED WITH A 0.20-CHORD, SEALED GAP, PLAIN AILERON OF NORMAL PROFILE. q = 30 lb/sq ft. R = 3,800,000

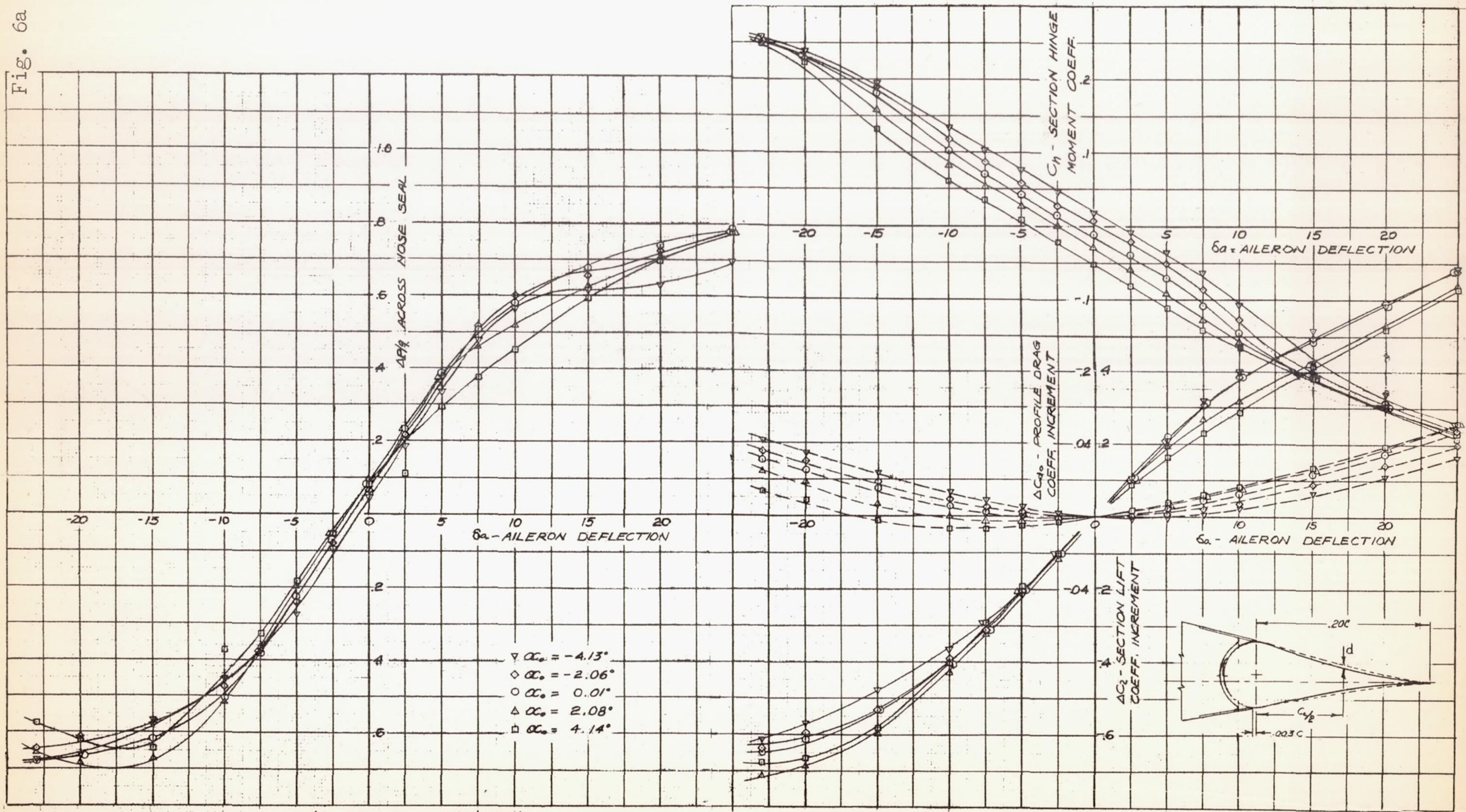

(1 block = 10/40")

FIGURE 6a.- SECTION AERODYNAMIC CHARACTERISTICS OF AN NACA 66, 2-216 (a = 0.6) AIRFOIL EQUIPPED WITH A 0.20-CHORD, SEALED GAP, PLAIN AILERON OF THINNED PROFILE. $d = -0.009\,c_a$. $q = 180$ lb/sq ft. $R = 9{,}000{,}000$

Fig. 6b

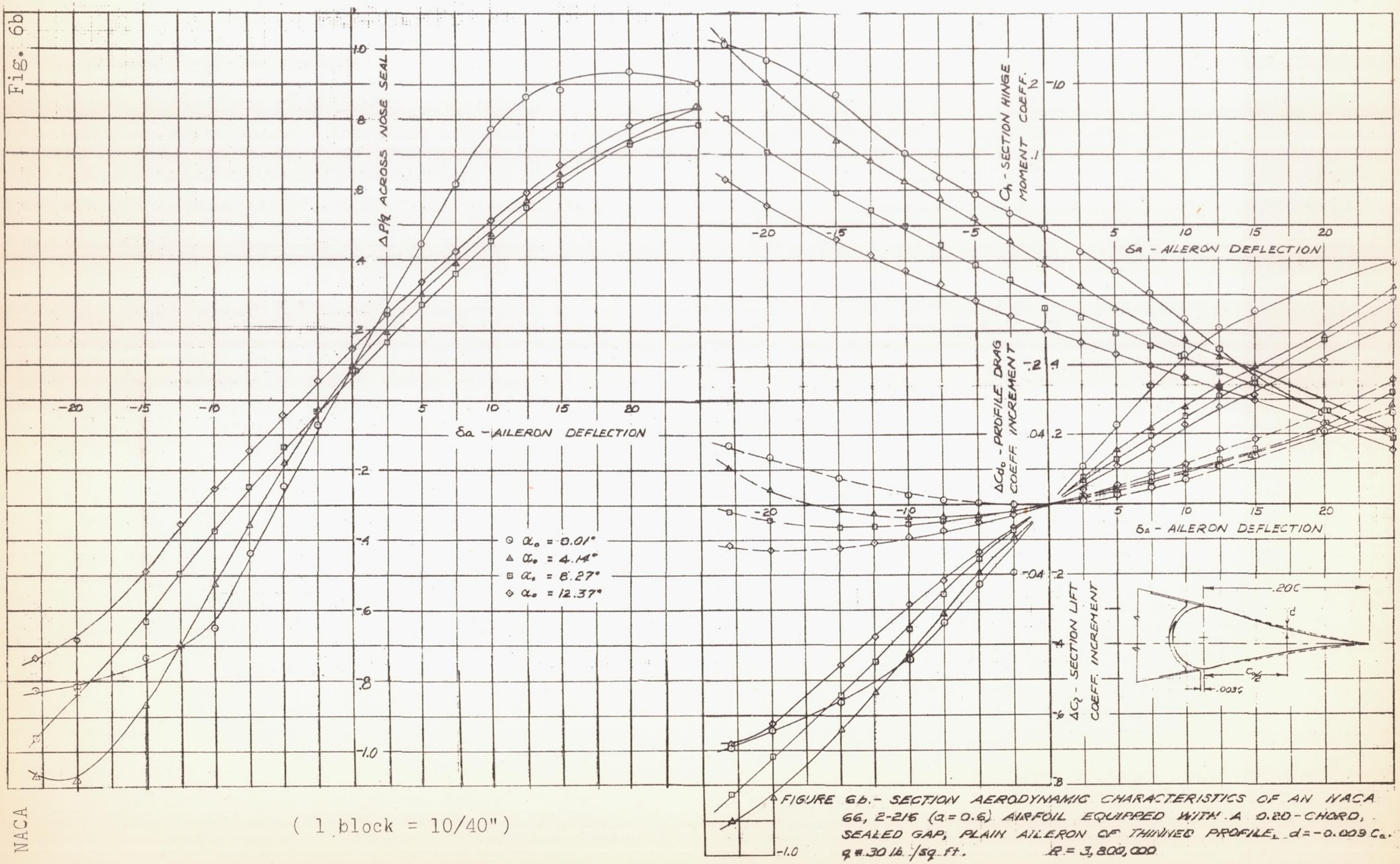

FIGURE 6b.- SECTION AERODYNAMIC CHARACTERISTICS OF AN NACA 66, 2-216 (a=0.6) AIRFOIL EQUIPPED WITH A 0.20-CHORD, SEALED GAP, PLAIN AILERON OF THINNED PROFILE, d=-0.009 C_a. q = 30 lb./sq. ft. R = 3,800,000

NACA

(1 block = 10/40")

A-55

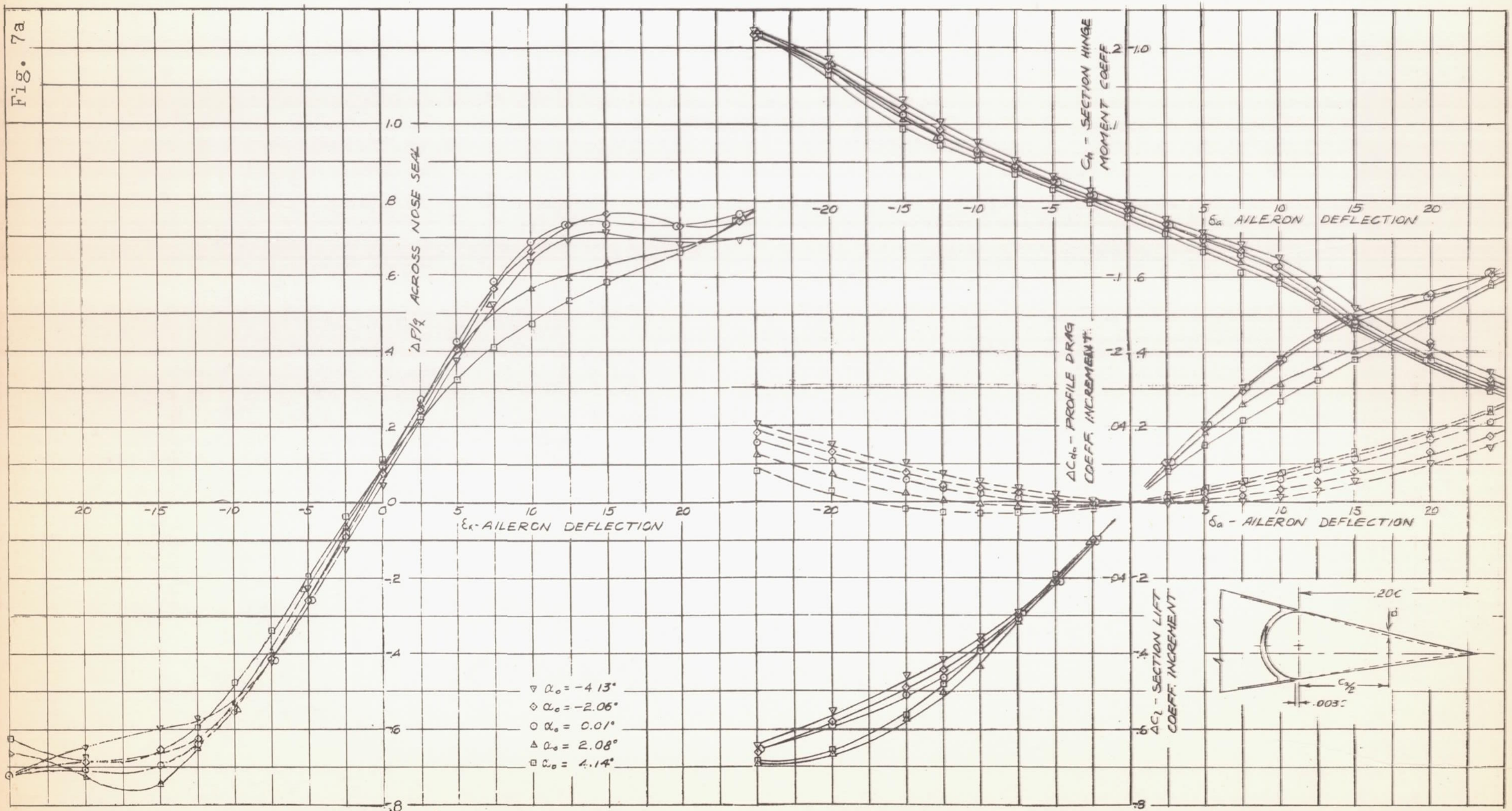

(1 block = 10/40")

FIGURE 7a.– SECTION AERODYNAMIC CHARACTERISTICS OF AN NACA 66, 2-216 (a=0.6) AIRFOIL EQUIPPED WITH A 0.20-CHORD, SEALED GAP, PLAIN AILERON OF INTERMEDIATE-THICKENED PROFILE, $d = 0.009\ c_a$. $q = 180$ lb/sq ft. $R = 9,000,000$

NACA

A-55

Fig. 7b

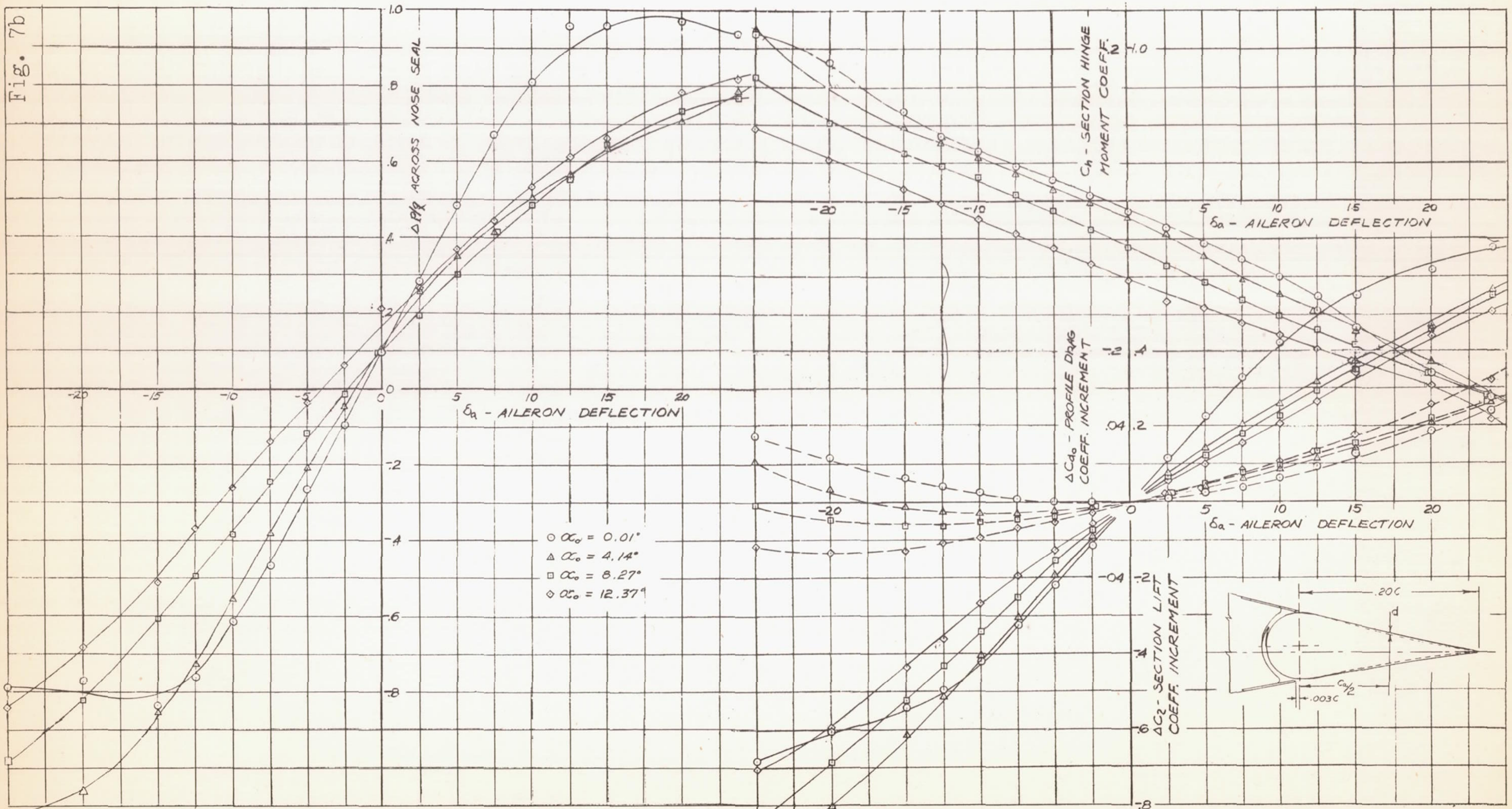

FIGURE 7b.- SECTION AERODYNAMIC CHARACTERISTICS OF AN NACA 66, 2-216 (a=0.6) AIRFOIL EQUIPPED WITH A 0.20-CHORD, SEALED GAP, PLAIN AILERON OF INTERMEDIATE-THICKENED PROFILE, d= 0.003 C_a. q=30 lb/sq ft. R= 3,800,000

NACA

(1 block = 10/40")

A-55

A-55

(1 block = 10/40")

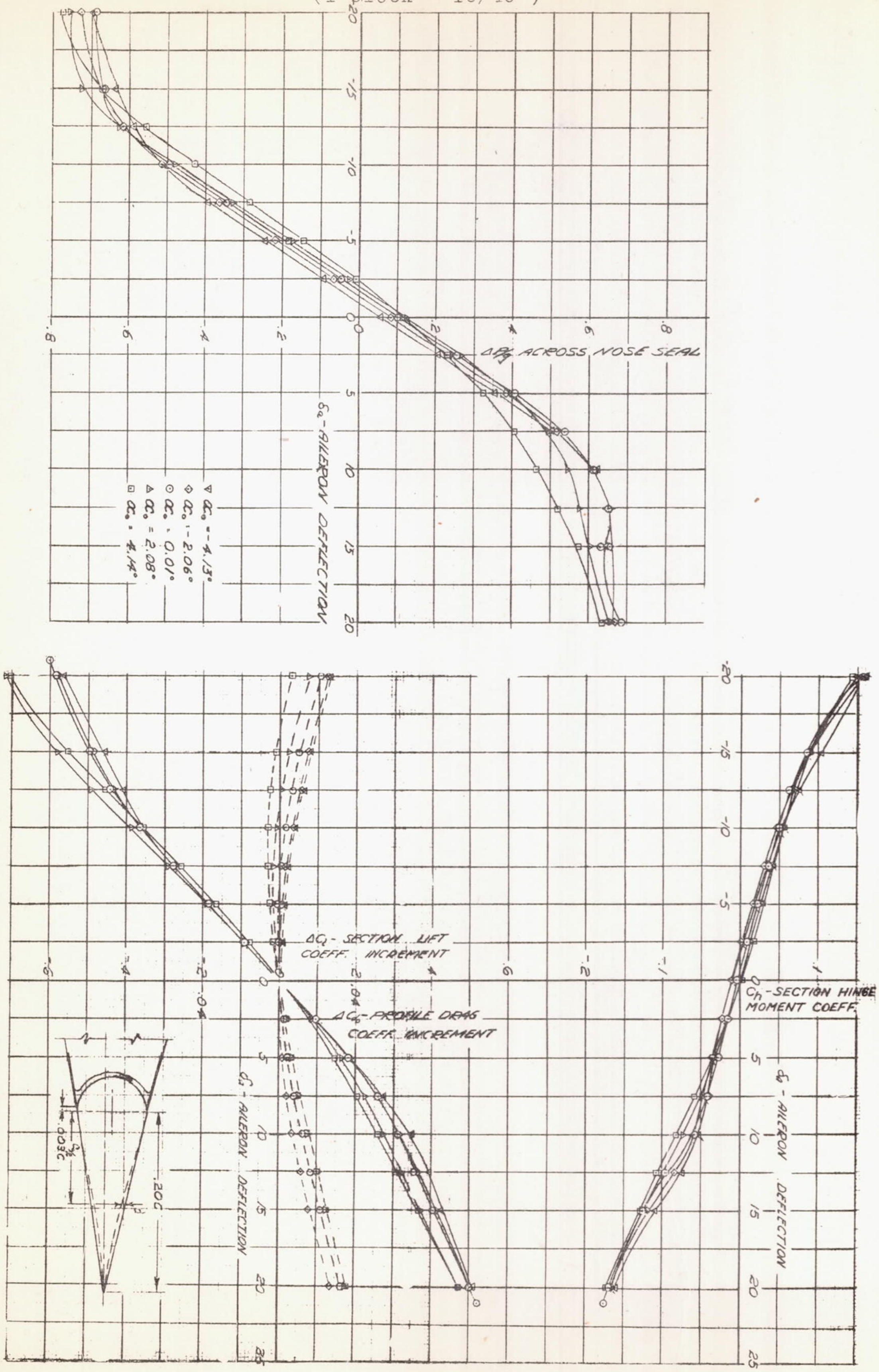

FIGURE 8a.- SECTION AERODYNAMIC CHARACTERISTICS OF AN NACA 66, 2-216 (a = 0.6) AIRFOIL EQUIPPED WITH A 0.20-CHORD, SEALED GAP, PLAIN AILERON OF STRAIGHT-SIDED PROFILE. d = 0.018 c_a. q = 180 lb/sq ft. R = 9,000,000

A-55

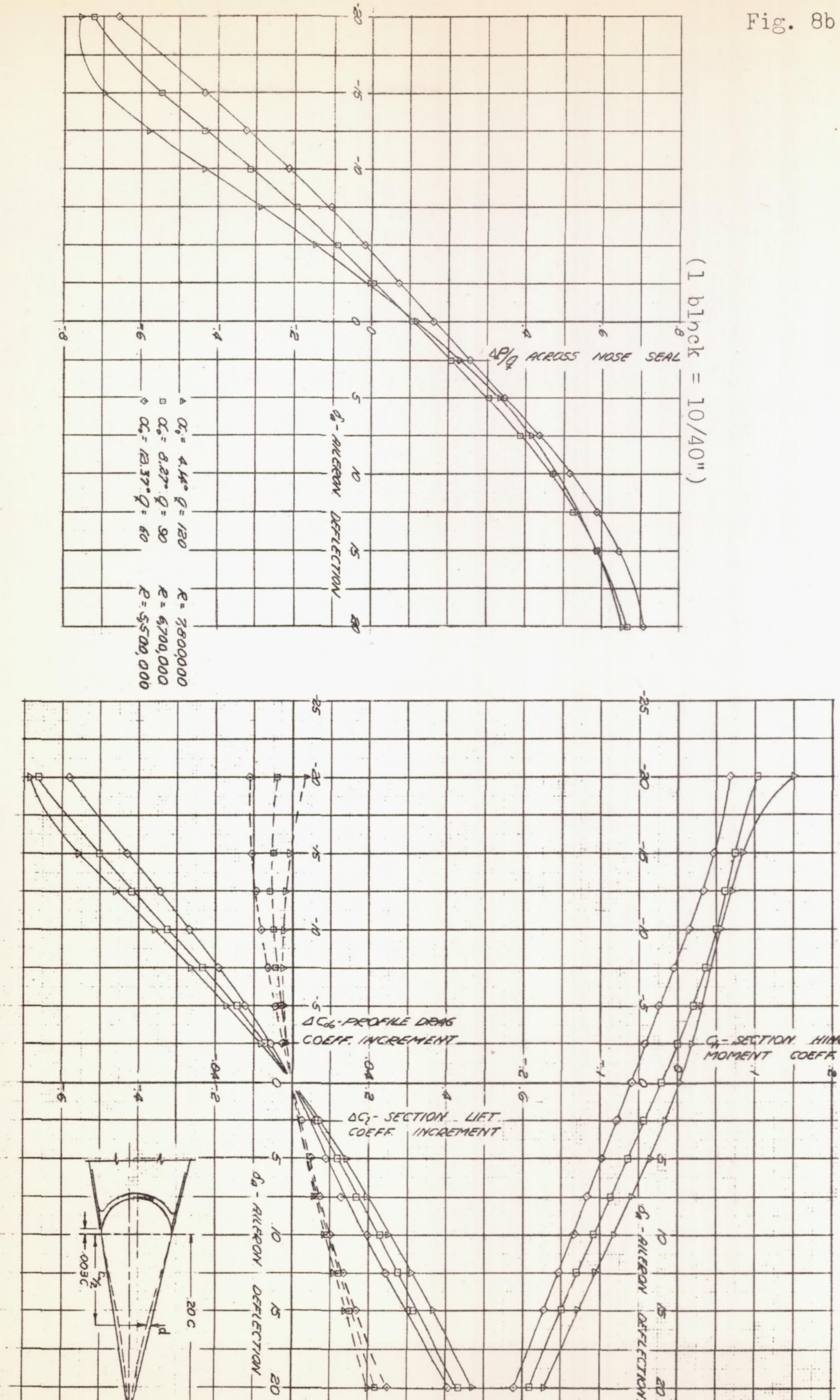

FIGURE 8b. - SECTION AERODYNAMIC CHARACTERISTICS OF AN NACA 66, 2-216 (a=0.6) AIRFOIL EQUIPPED WITH A 0.20-CHORD, SEALED GAP, PLAIN AILERON OF STRAIGHT-SIDED PROFILE, $d = 0.018\ C_a$.

Fig. 9a

(1 block = 10/40")

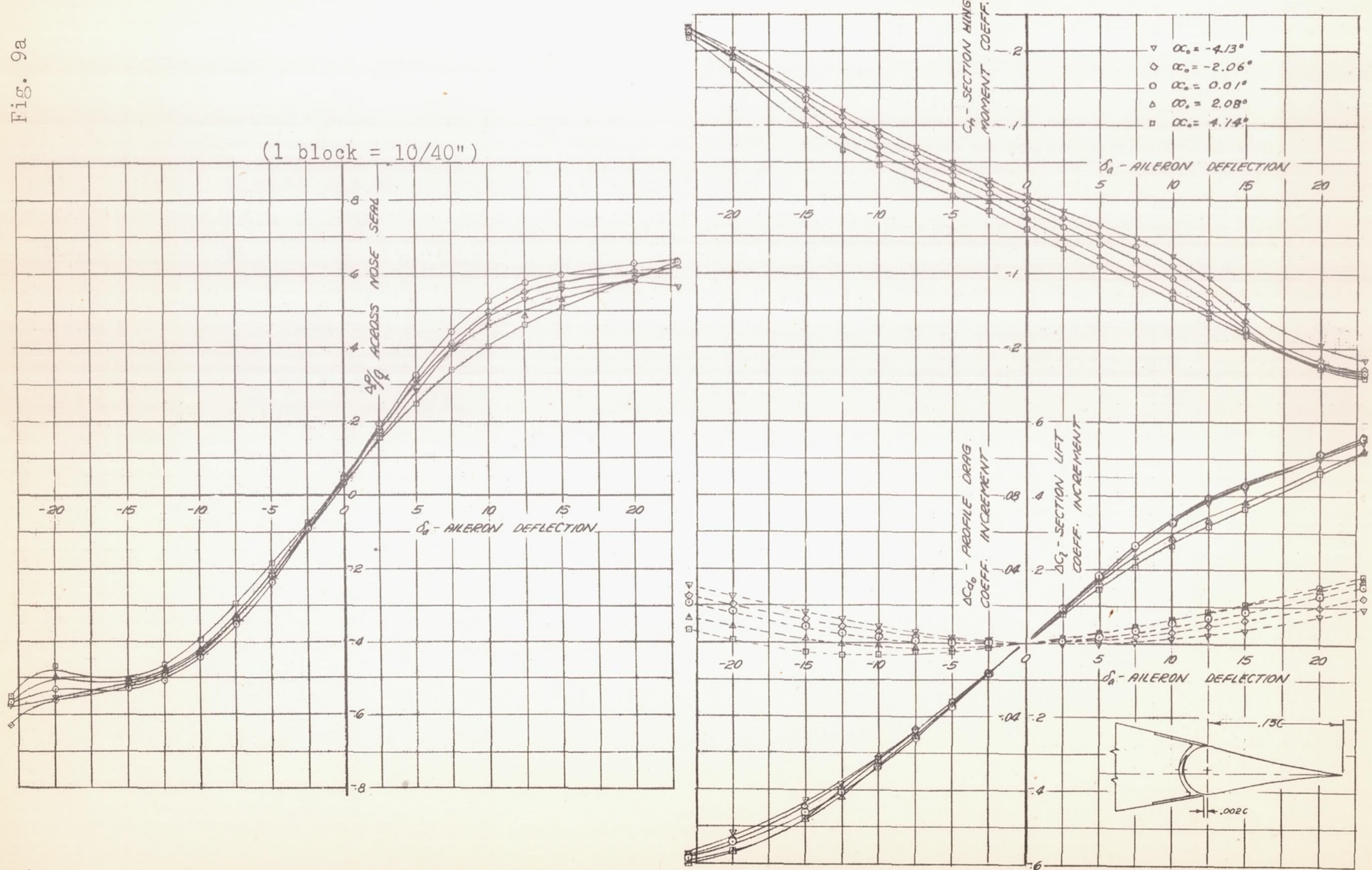

FIGURE 9a.- SECTION AERODYNAMIC CHARACTERISTICS OF AN NACA 66, 2-216 (a = 0.6) AIRFOIL EQUIPPED WITH A 0.15-CHORD, SEALED GAP, PLAIN AILERON OF NORMAL PROFILE. q = 180 lb/sq ft. R = 9,000,000

NACA

National Advisory Committee for Aeronautics

A-55

(1 block = 10/40")

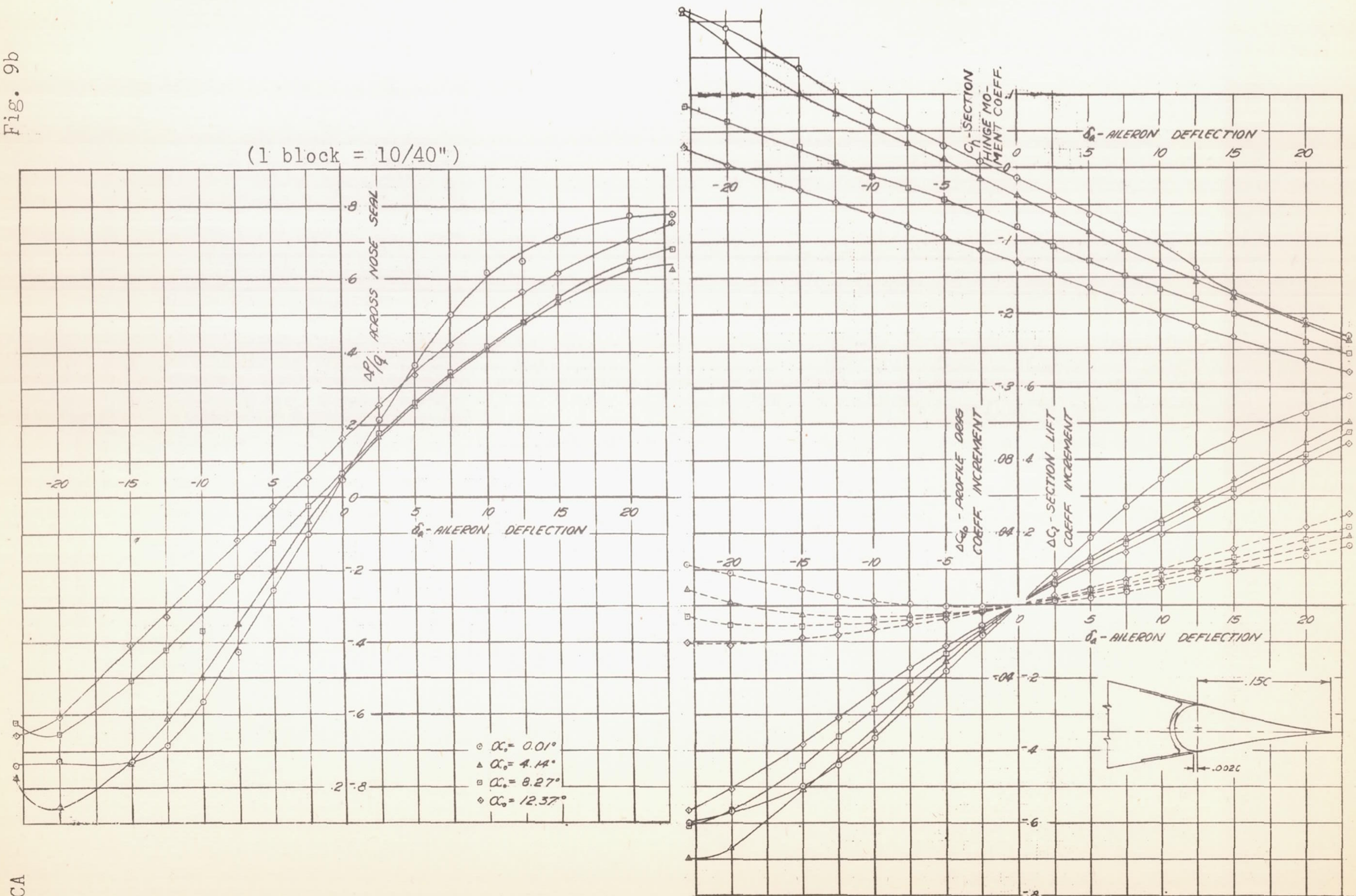

FIGURE 9b.- SECTION AERODYNAMIC CHARACTERISTICS OF AN NACA 66, 2-216 (a = 0.6) AIRFOIL EQUIPPED WITH A 0.15-CHORD, SEALED GAP, PLAIN AILERON OF NORMAL PROFILE. q = 30 lb./sq. ft. R = 3,800,000

(1 block = 10/40")

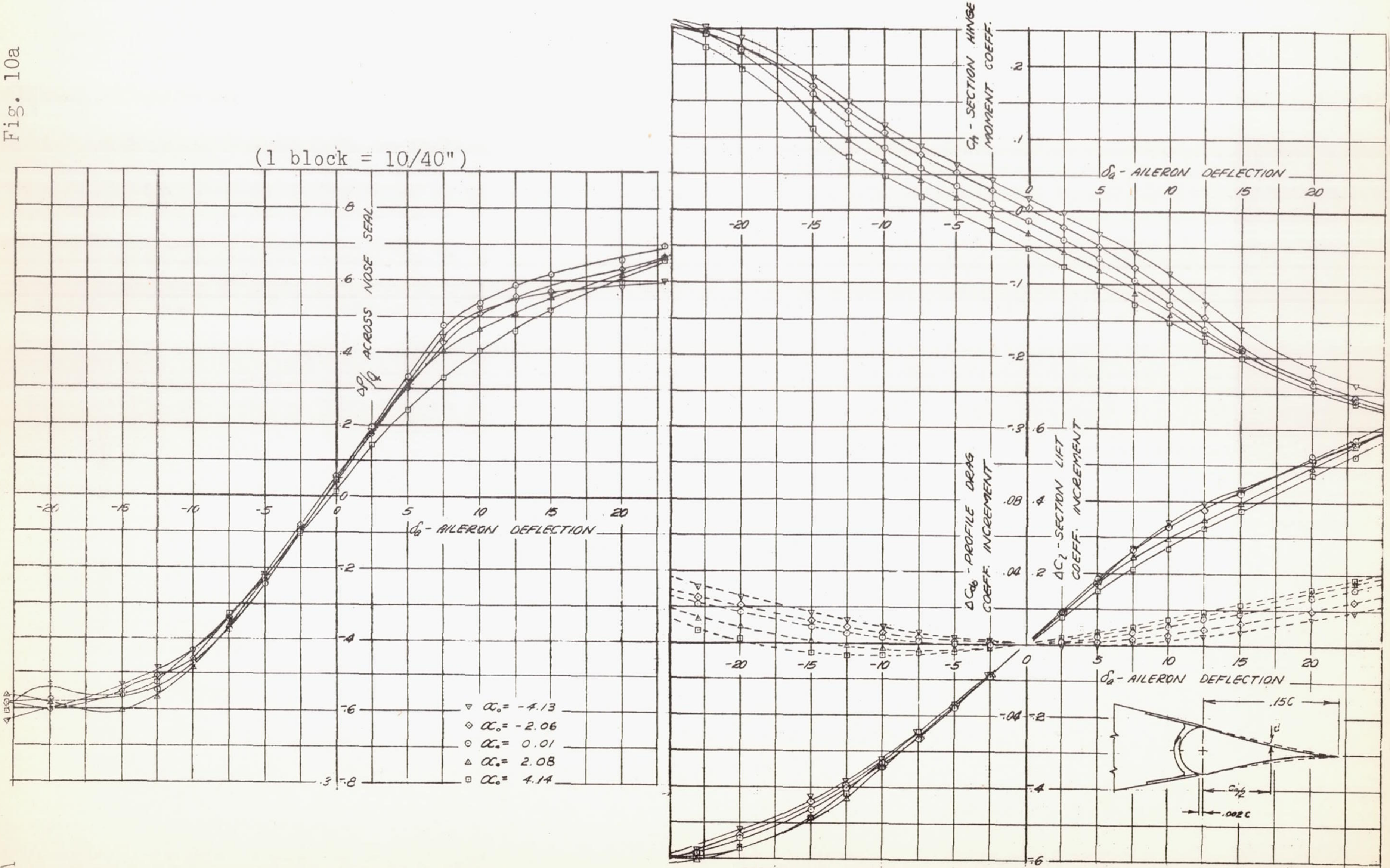

FIGURE 10a.- SECTION AERODYNAMIC CHARACTERISTICS OF AN NACA 66, 2-216 (a = 0.6) AIRFOIL EQUIPPED WITH A 0.15-CHORD, SEALED GAP, PLAIN AILERON OF THINNED PROFILE, d = -0.012 C_a. q = 180 lb/sq ft. R = 9,000,000

Fig. 10b

(1 block = 10/40")

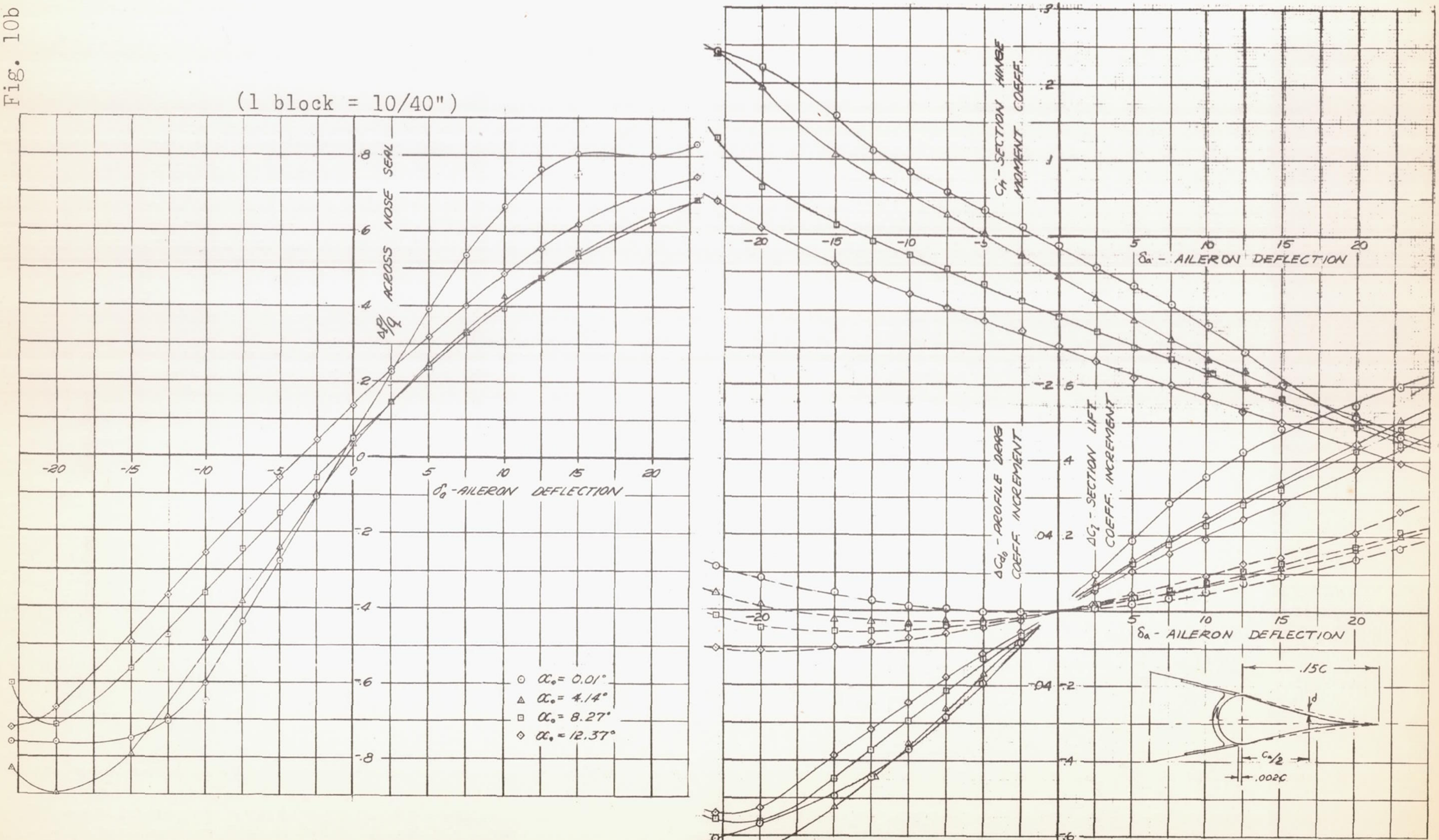

FIGURE 10b.- SECTION AERODYNAMIC CHARACTERISTICS OF AN NACA 66, 2-216 (a=0.6) AIRFOIL EQUIPPED WITH A 0.15-CHORD, SEALED GAP, PLAIN AILERON OF THINNED PROFILE. q = 30 lb./sq ft. R = 3,800,000 $d = -0.012\ C_a$.

NACA

Fig. 11a

(1 block = 10/40")

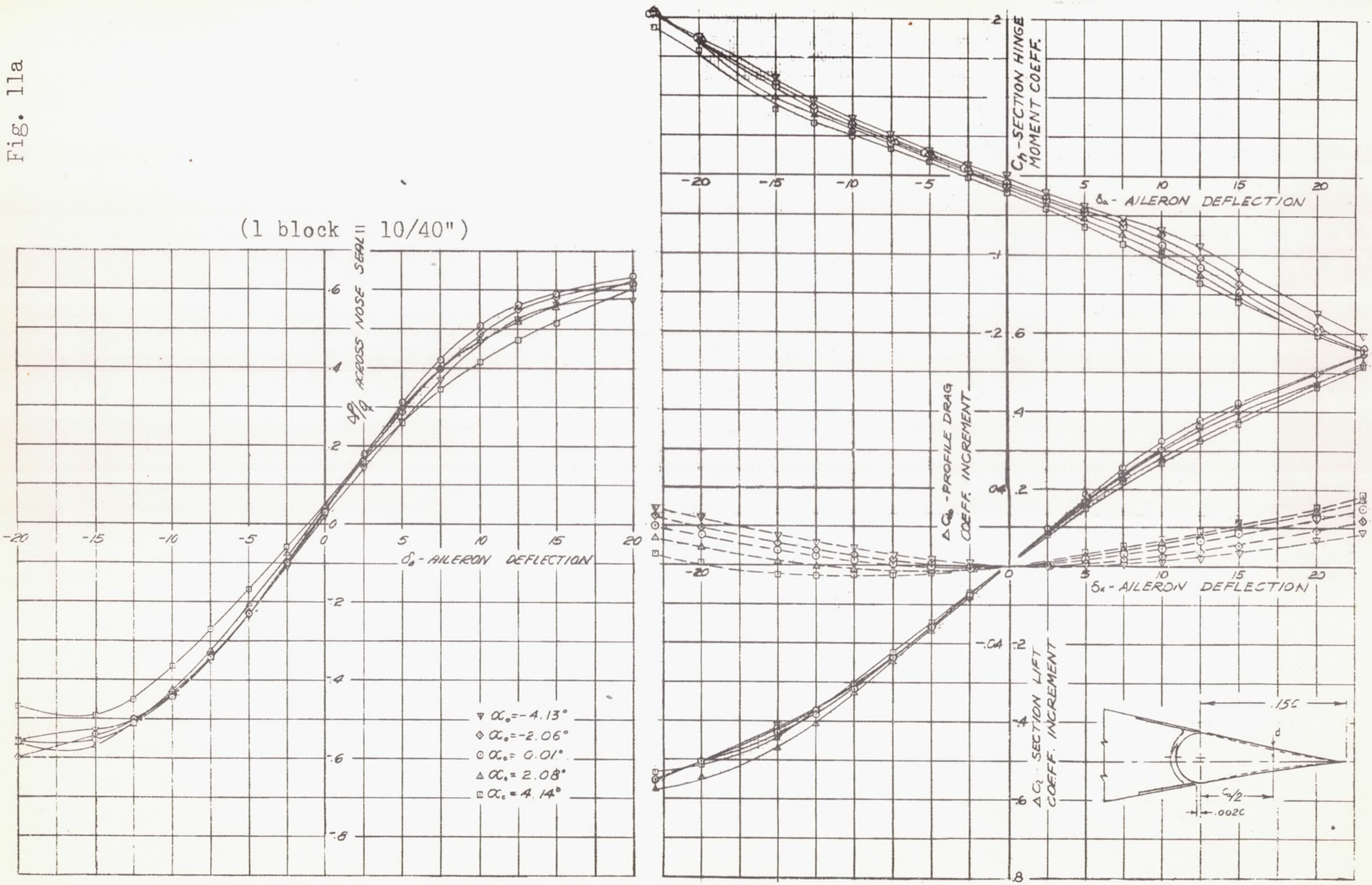

FIGURE 11a.- SECTION AERODYNAMIC CHARACTERISTICS OF AN NACA 66, 2-216 (a = 0.6) AIRFOIL EQUIPPED WITH A 0.15-CHORD, SEALED GAP, PLAIN AILERON OF INTERMEDIATE THICKENED PROFILE, $d = 0.010\,c_a$.
$q = 180$ lb/sq ft $R = 9,000,000$

NACA

Fig. 11b

(1 block = 10/40")

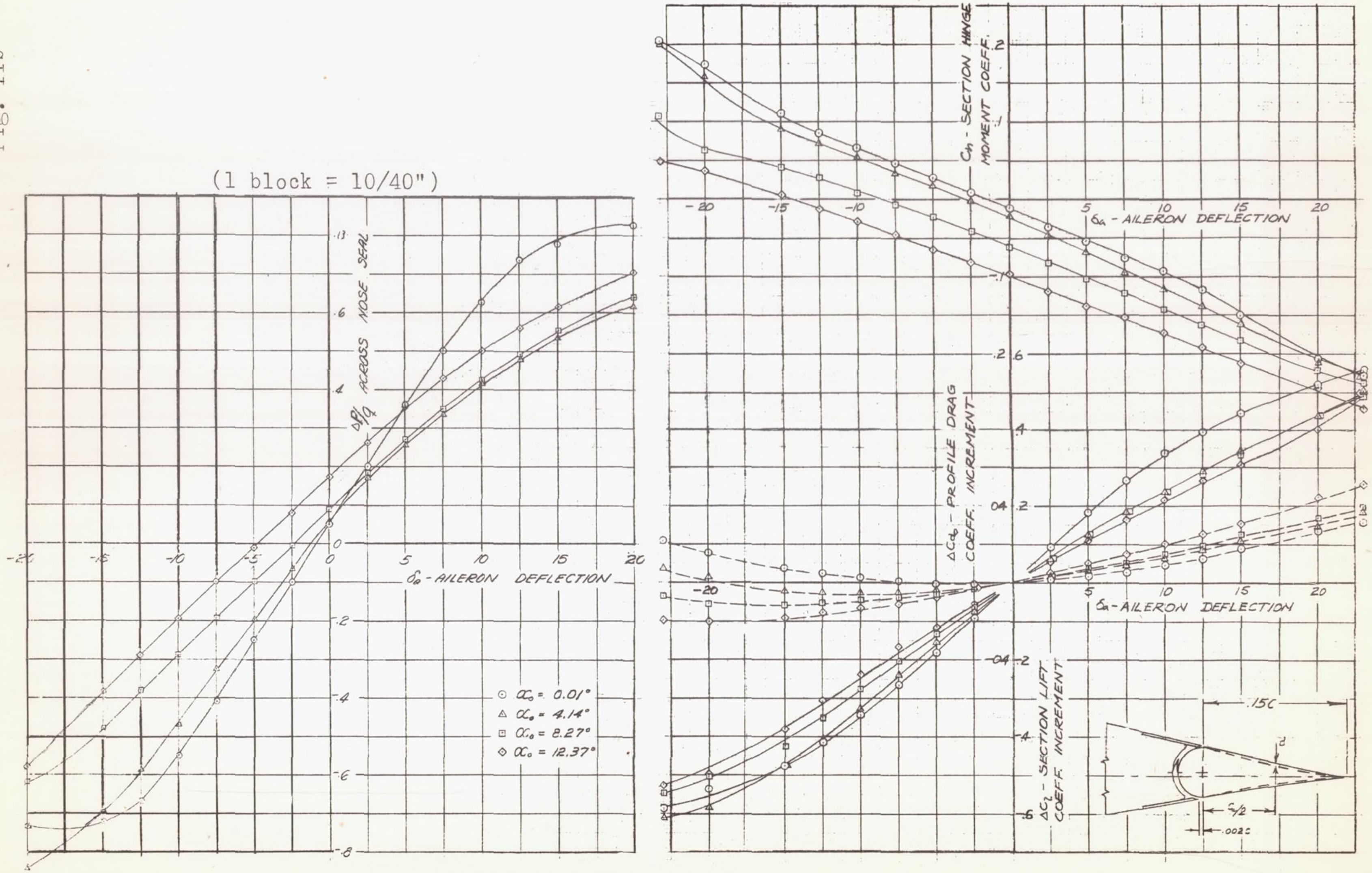

FIGURE 11b.- SECTION AERODYNAMIC CHARACTERISTICS OF AN NACA 66, 2-216 (a=0.6) AIRFOIL EQUIPPED WITH A 0.15-CHORD, SEALED GAP, PLAIN AILERON OF INTERMEDIATE THICKENED PROFILE, d=0.010 C_a.
q = 30 lb /sq ft. R = 3,800,000

NACA

Fig. 12a

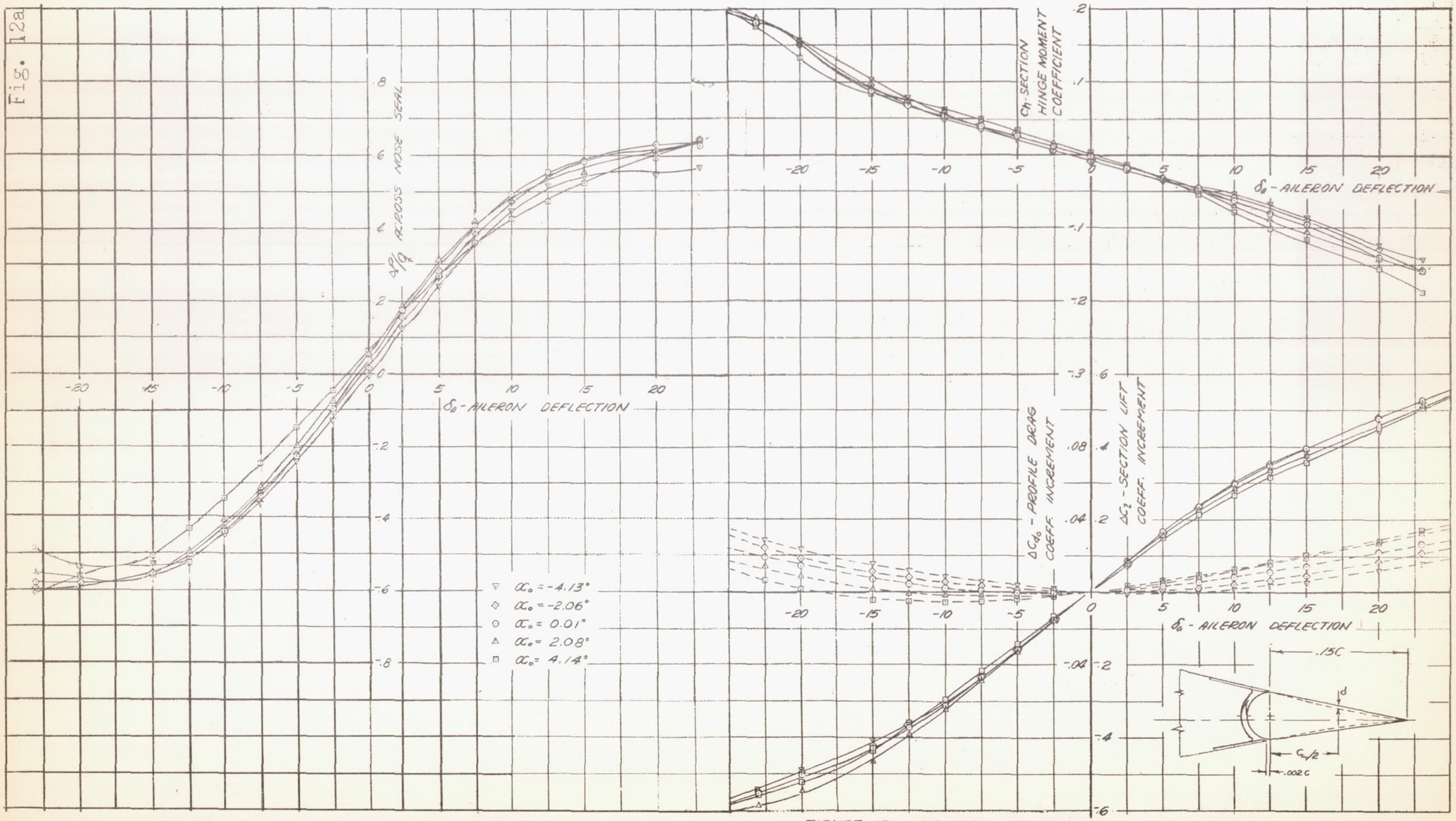

(1 block = 10/40")

FIGURE 12a.-SECTION AERODYNAMIC CHARACTERISTICS OF AN NACA 66, 2-216 (a=0.6) AIRFOIL EQUIPPED WITH A 0.15-CHORD, SEALED GAP, PLAIN AILERON OF STRAIGHT-SIDED PROFILE, $d=0.019\ C_a$. $q=180$ lb/sq ft. $R=9{,}000{,}000$.

NACA

NACA

Fig. 12b

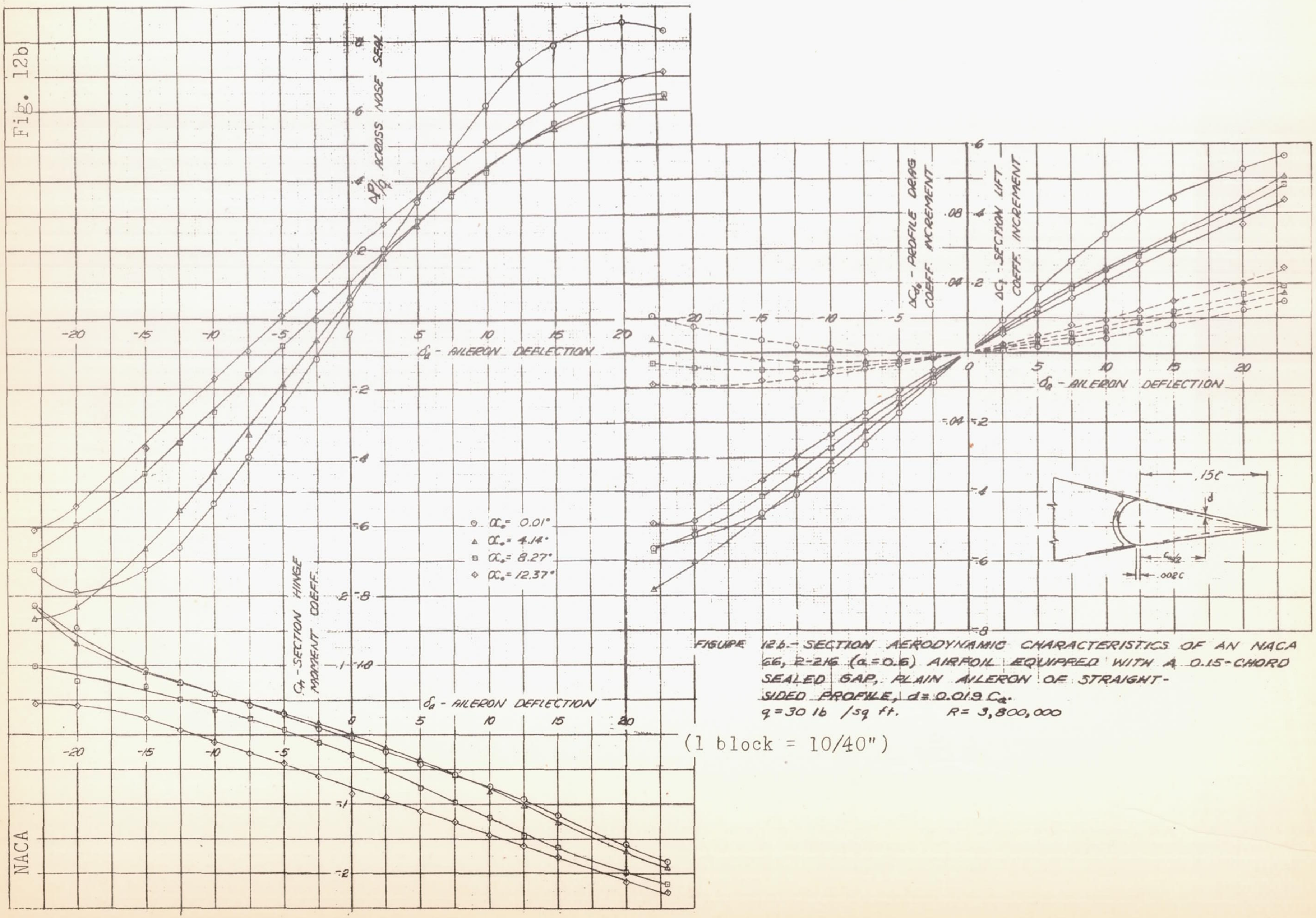

FIGURE 12b.- SECTION AERODYNAMIC CHARACTERISTICS OF AN NACA 66, 2-216 (a=0.6) AIRFOIL EQUIPPED WITH A 0.15-CHORD SEALED GAP, PLAIN AILERON OF STRAIGHT-SIDED PROFILE, d=0.019 C_a.
q = 30 lb/sq ft. R = 3,800,000

(1 block = 10/40")

A-55

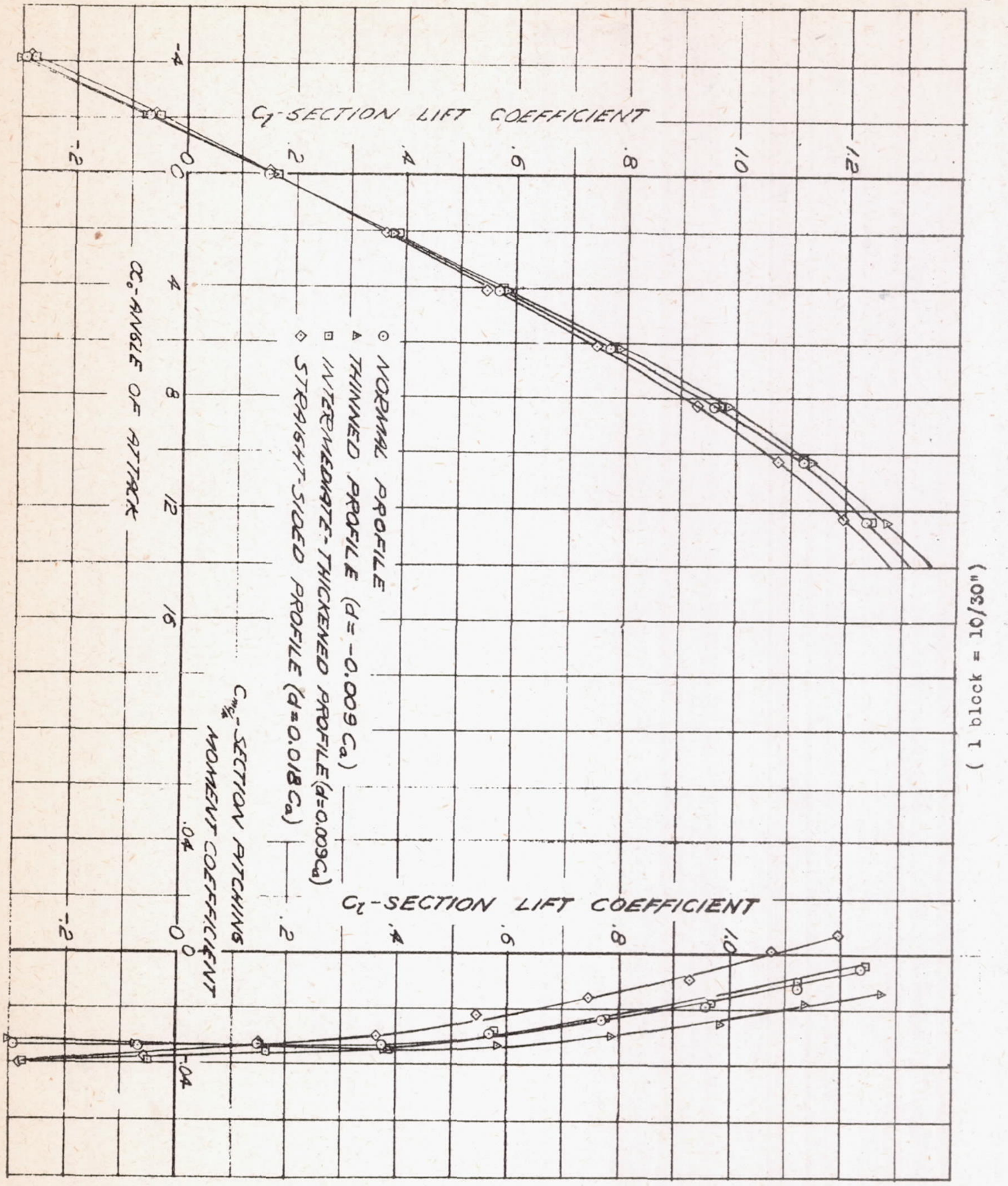

FIGURE 13a.- THE EFFECT OF MODIFICATIONS OF THE AILERON PROFILE ON THE SECTION AERODYNAMIC CHARACTERISTICS OF AN NACA 66, 2-216 (a = 0.6) AIRFOIL EQUIPPED WITH A 0.20-CHORD, SEALED GAP, PLAIN AILERON. AILERON UNDEFLECTED; q = 150 lb /sq ft. R = 8,200,000

A-55

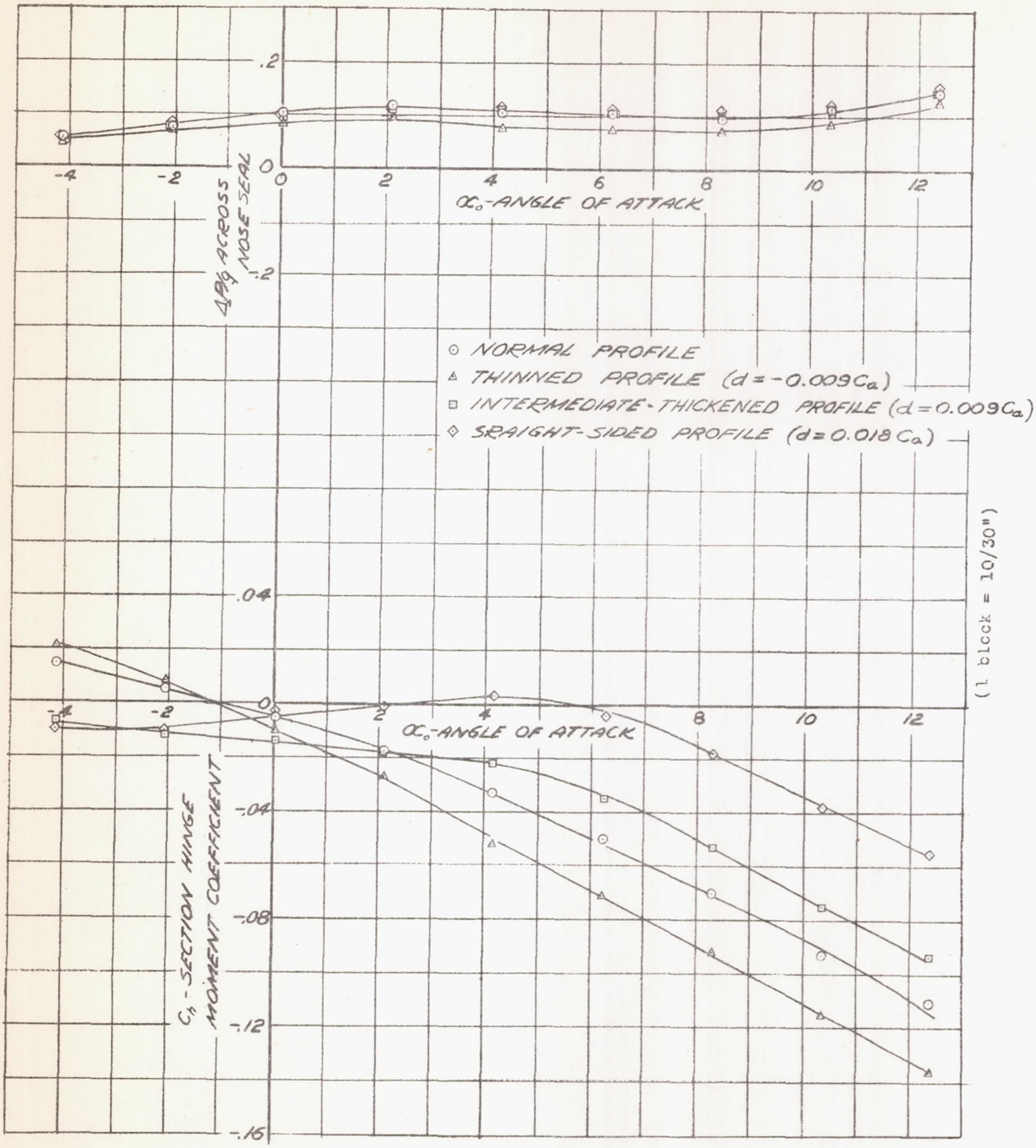

FIGURE 13b.- THE EFFECT OF MODIFICATIONS OF THE AILERON PROFILE ON THE SECTION AERODYNAMIC CHARACTERISTICS OF AN NACA 66, 2-216 (a = 0.6) AIRFOIL EQUIPPED WITH A 0.20-CHORD, SEALED GAP, PLAIN AILERON. AILERON UNDEFLECTED; q = 150 lb /sq ft. R = 8,200,000.

A-55

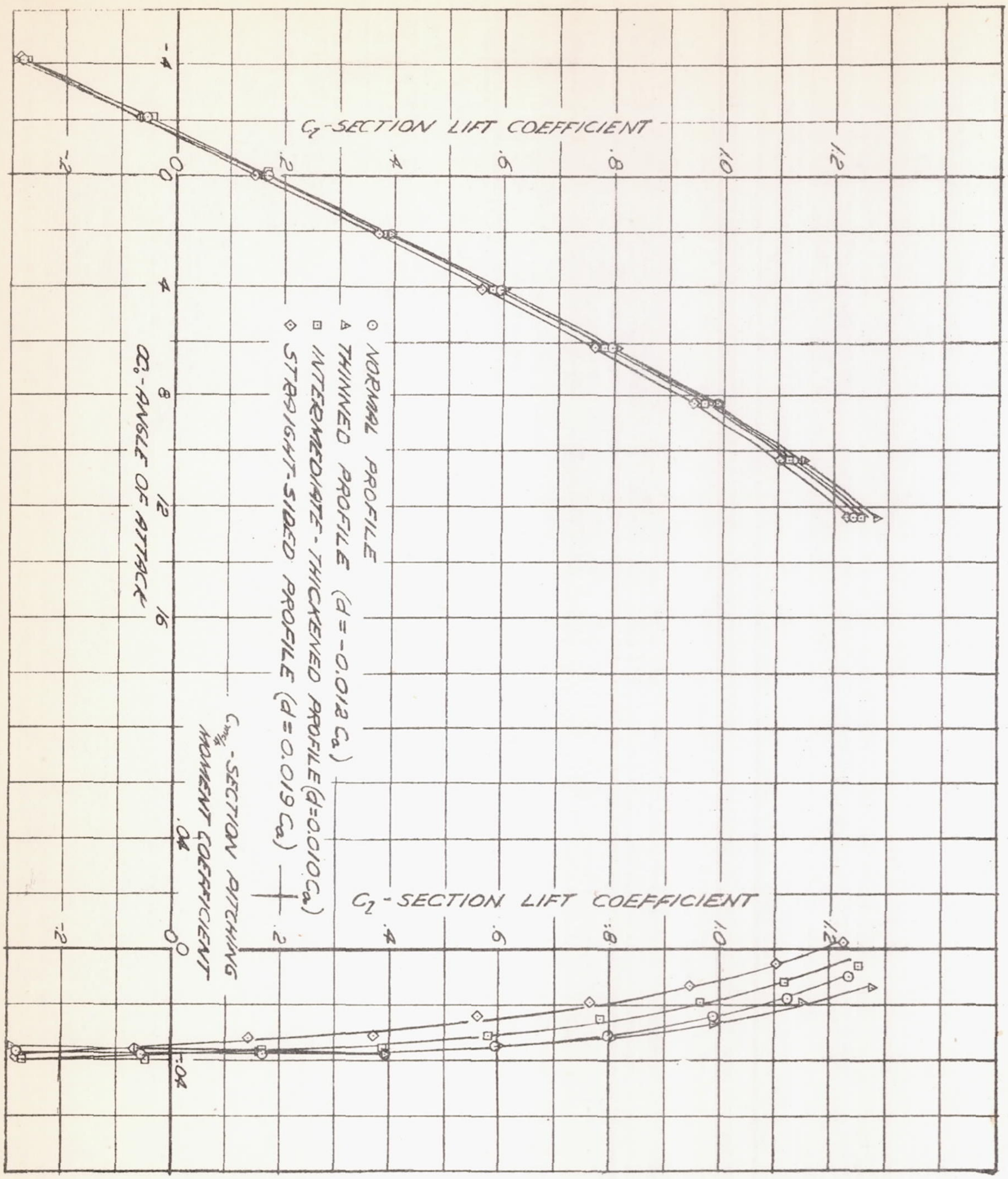

(1 block = 10/30")

FIGURE 14a.- THE EFFECT OF MODIFICATIONS OF THE AILERON PROFILE ON THE SECTION AERODYNAMIC CHARACTERISTICS OF AN NACA 66, 2-216 (a = 0.6) AIRFOIL EQUIPPED WITH A 0.15-CHORD, SEALED GAP, PLAIN AILERON. AILERON UNDEFLECTED; q = 150 lb. /sq ft.
R = 8,200,000

A-55

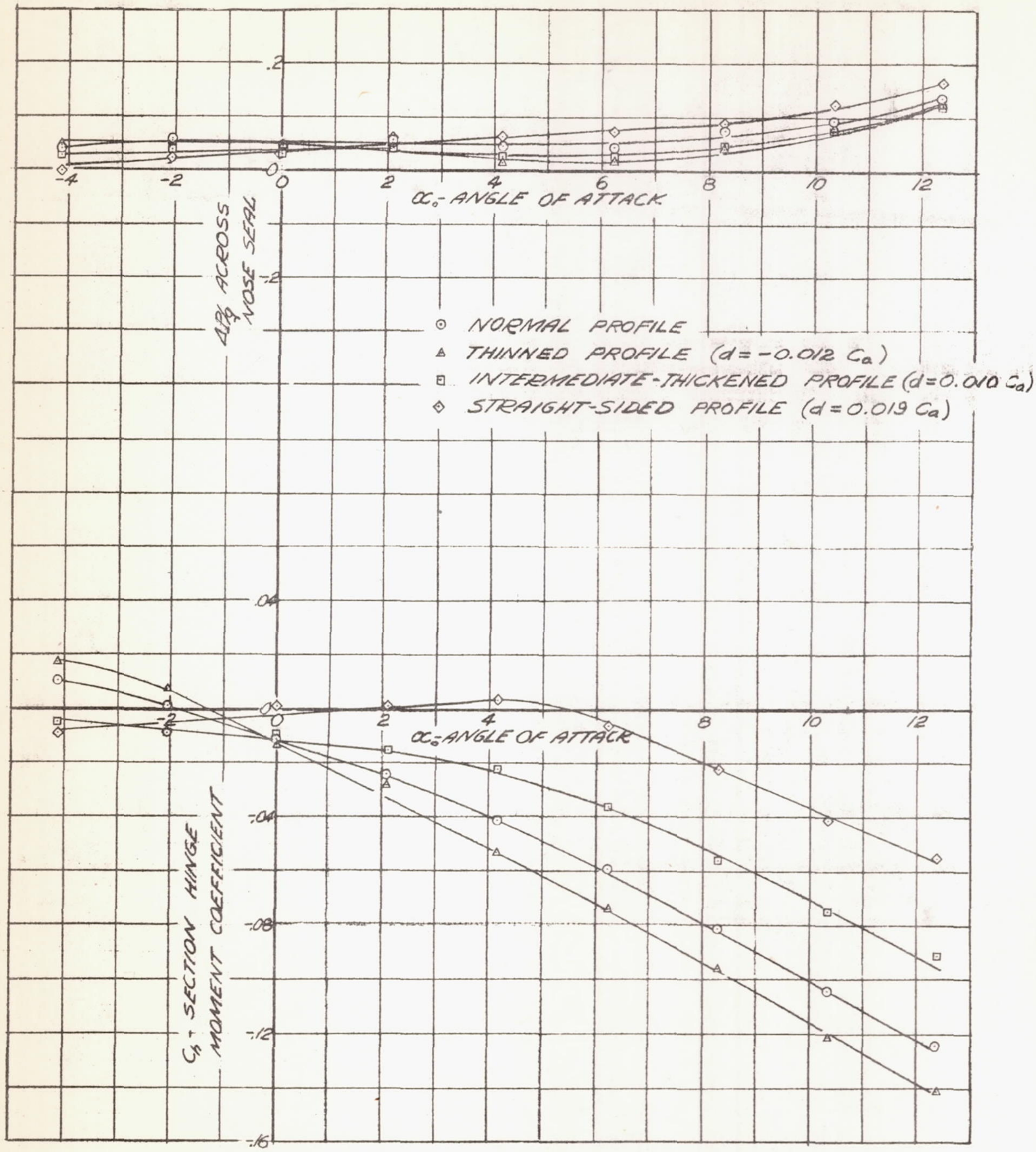

(1 block = 10/30")

FIGURE 14b.- THE EFFECT OF MODIFICATION OF THE AILERON PROFILE ON THE SECTION AERODYNAMIC CHARACTERISTICS OF AN NACA 66, 2-216 (a = 0.6) AIRFOIL EQUIPPED WITH A 0.15-CHORD, SEALED GAP, PLAIN AILERON. AILERON UNDEFLECTED; q = 150 lb /sq. ft. R = 8,200,000.

A-55

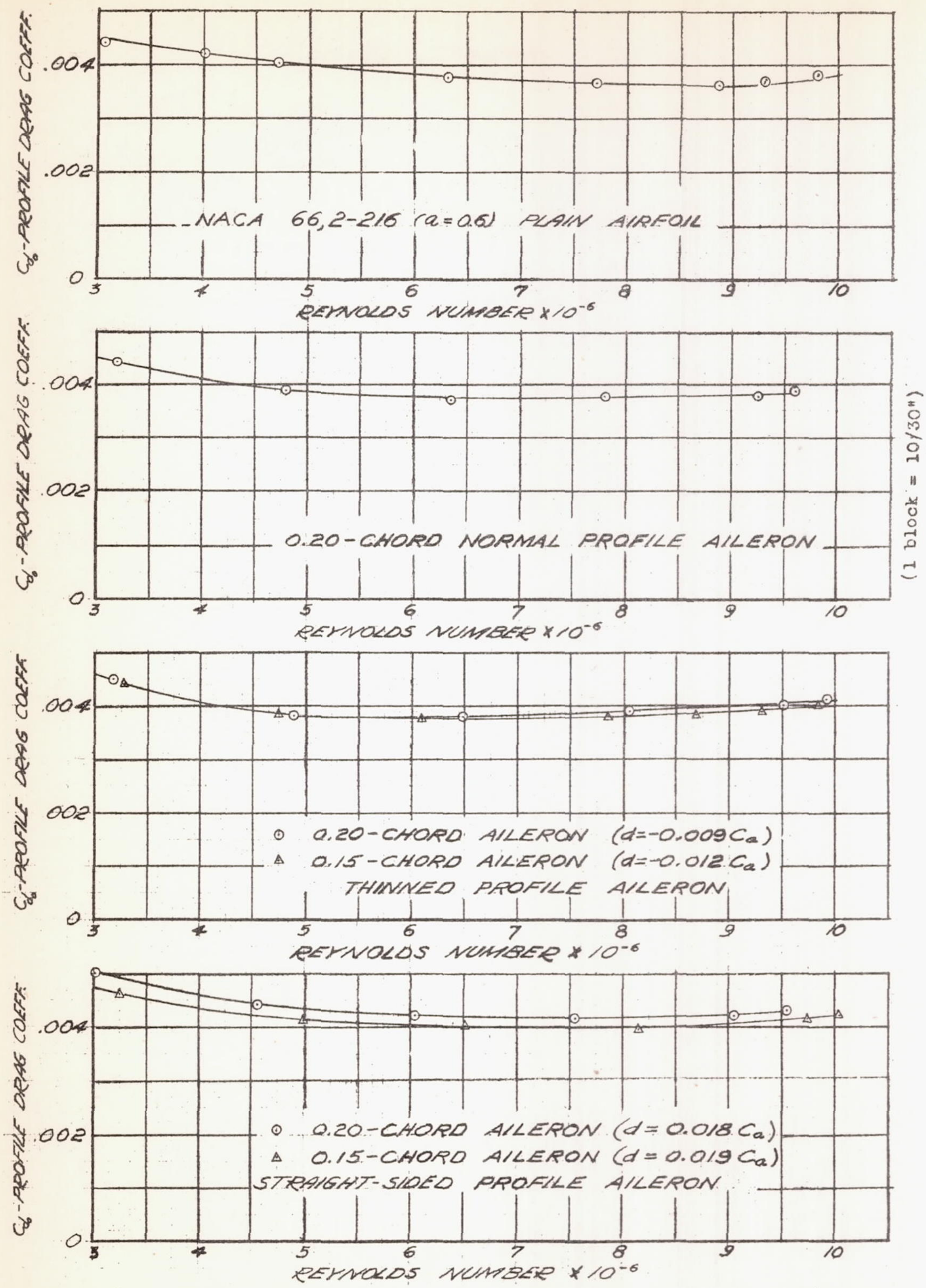

FIGURE 15.- THE EFFECT OF MODIFICATION OF THE AILERON PROFILE ON THE VARIATION OF SECTION PROFILE-DRAG COEFFICIENT WITH REYNOLDS NUMBER FOR AN NACA 66, 2-216 (a=0.6) AIRFOIL. AILERON UNDEFLECTED. $\alpha_0 = 0.51°$

A-55

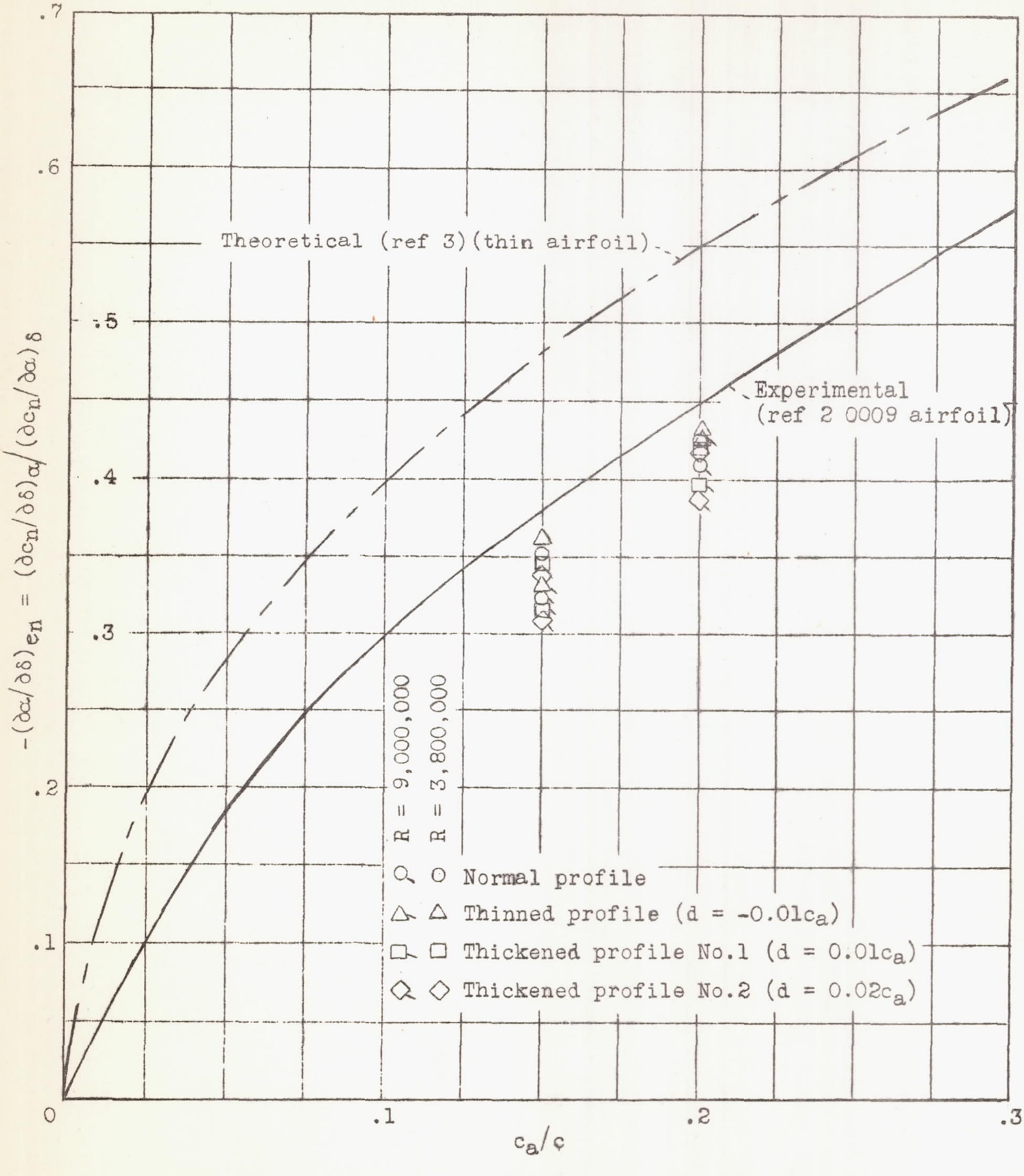

Figure 16.- The effect of modifications of the aileron profile on the aileron effectiveness parameter, $(\partial\alpha/\partial\delta)_{c_n}$ for an NACA 66,2-216 (a=0.6) airfoil equipped with sealed gap ailerons.

A-55

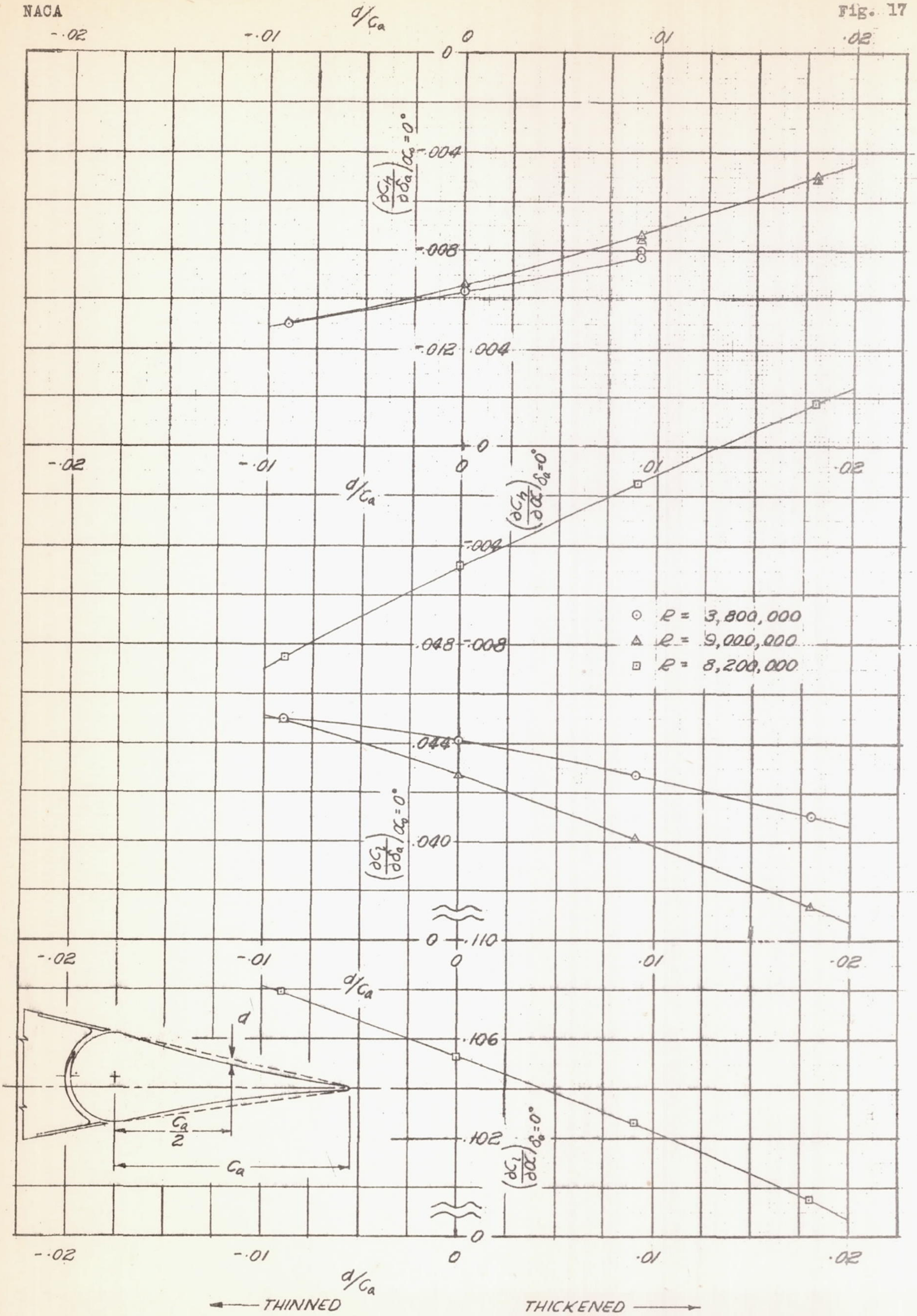

(1 block = 10/30")

FIGURE 17.- THE EFFECT OF MODIFICATIONS OF THE AILERON PROFILE ON THE SECTION PARAMETERS OF AN NACA 66,2-216 (a=0.6) AIRFOIL EQUIPPED WITH A 0.20-CHORD, SEALED GAP, PLAIN AILERON

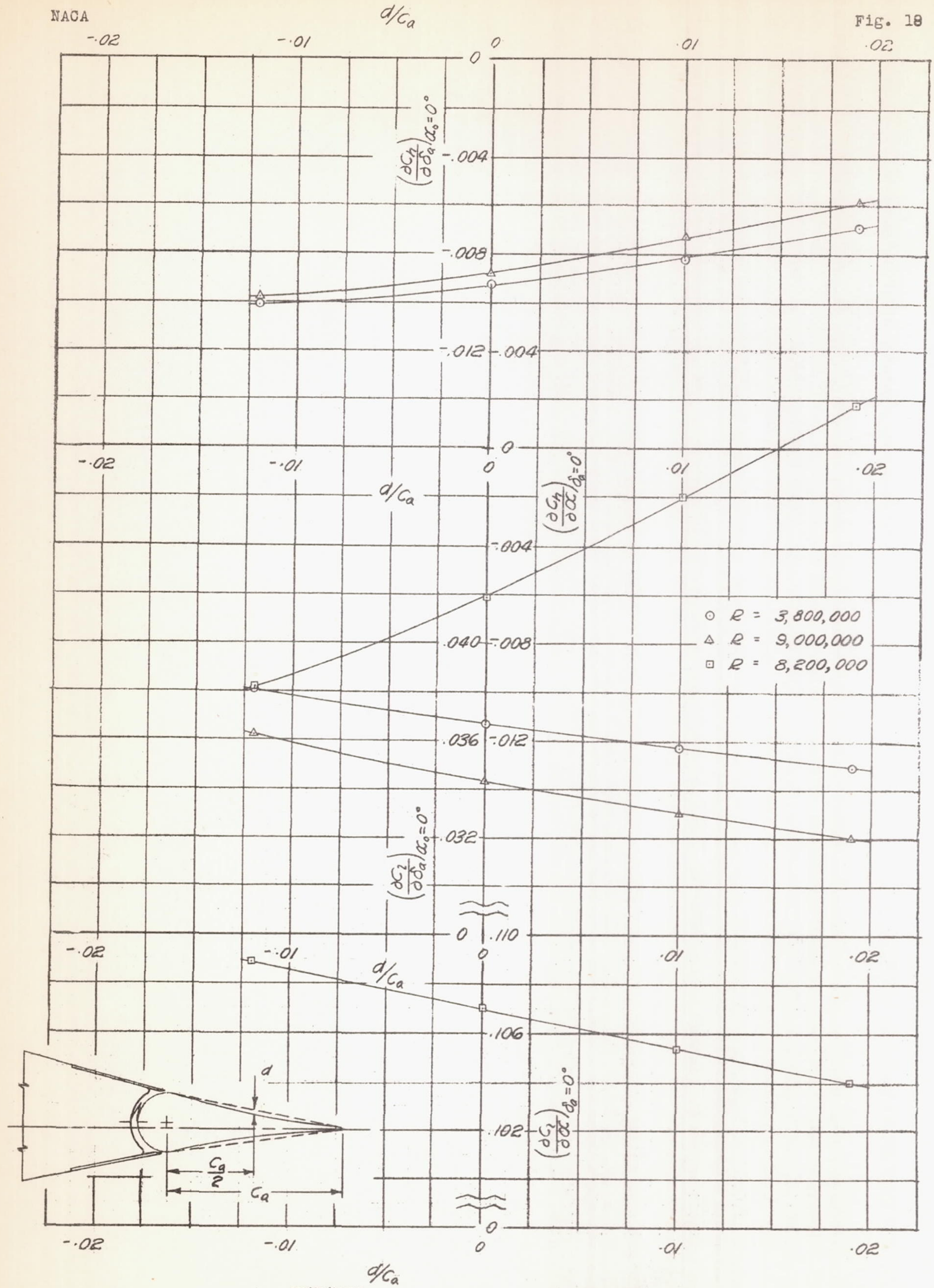

(1 block = 10/30")

FIGURE 18.- THE EFFECT OF MODIFICATIONS OF THE AILERON PROFILE ON THE SECTION PARAMETERS OF AN NACA 66,2-216 (a=0·6) AIRFOIL EQUIPPED WITH A 0·15-CHORD, SEALED GAP, PLAIN AILERON

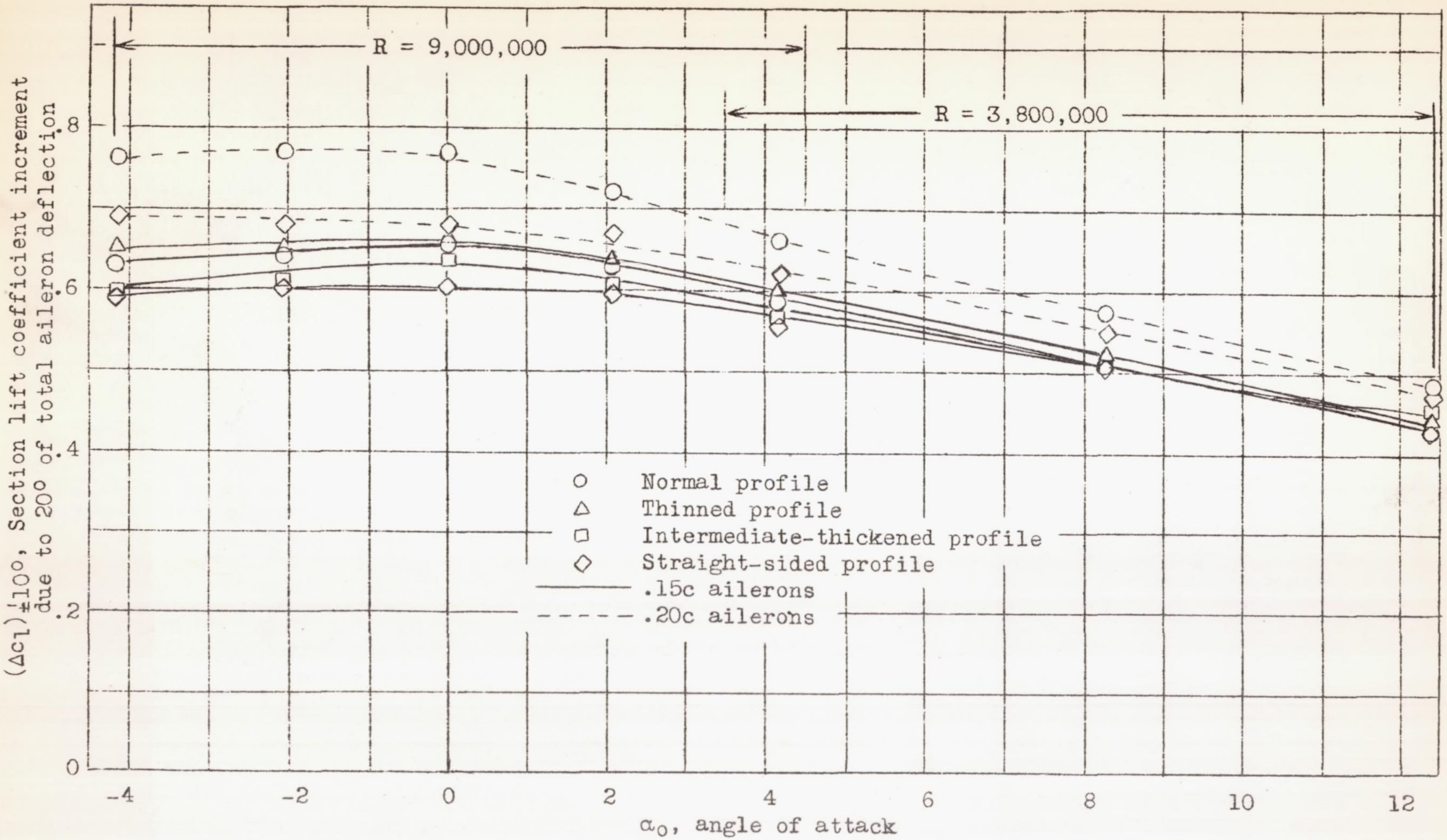

Figure 19.- The effect of modifications of the aileron profile on the aileron effectiveness for an NACA 66,2-216 (a=0.6) airfoil equipped with a sealed gap, plain aileron.

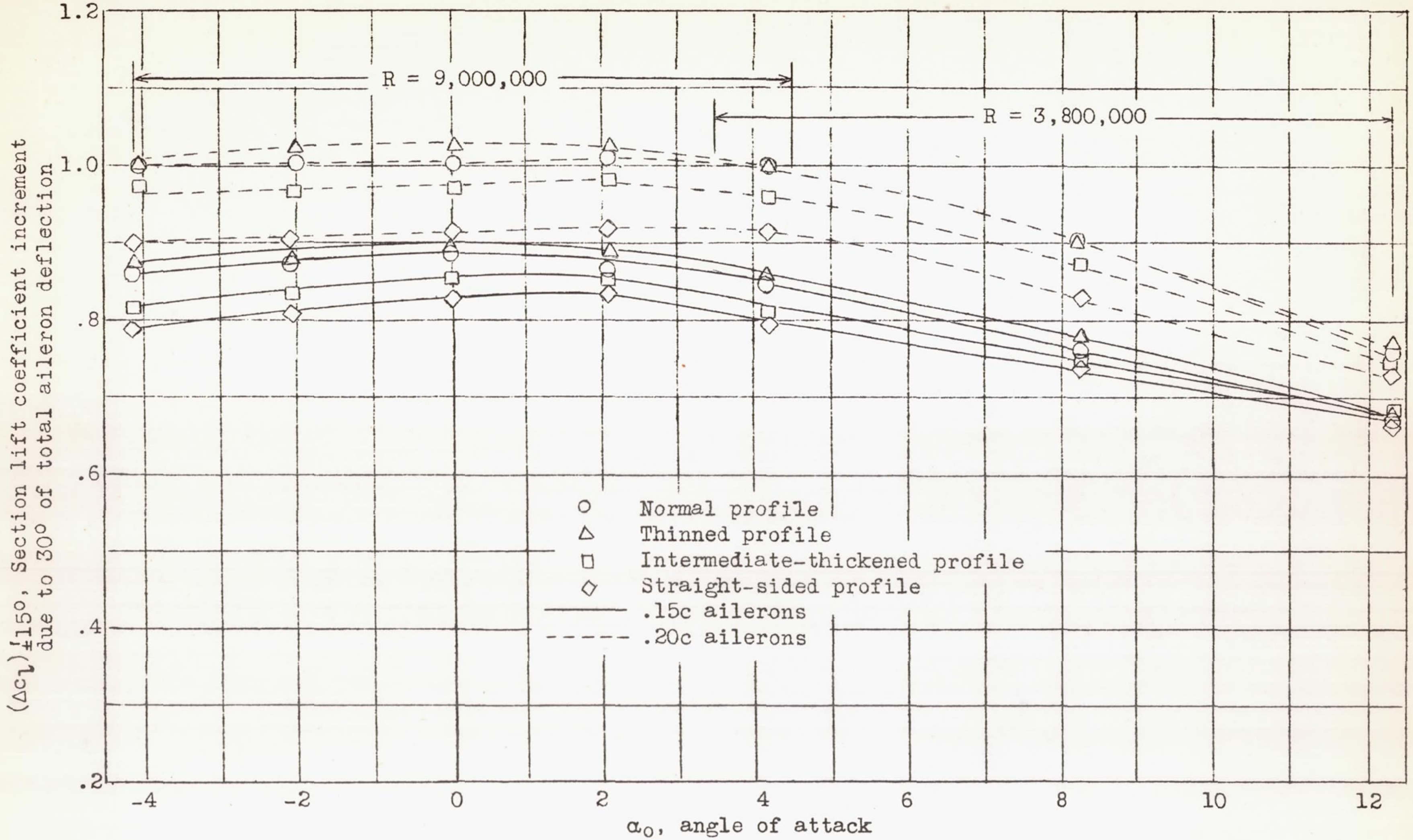

Figure 20.- The effect of modifications of the aileron profile on the aileron effectiveness for an NACA 66,2-216 (a=0.6) airfoil equipped with a sealed gap, plain aileron.

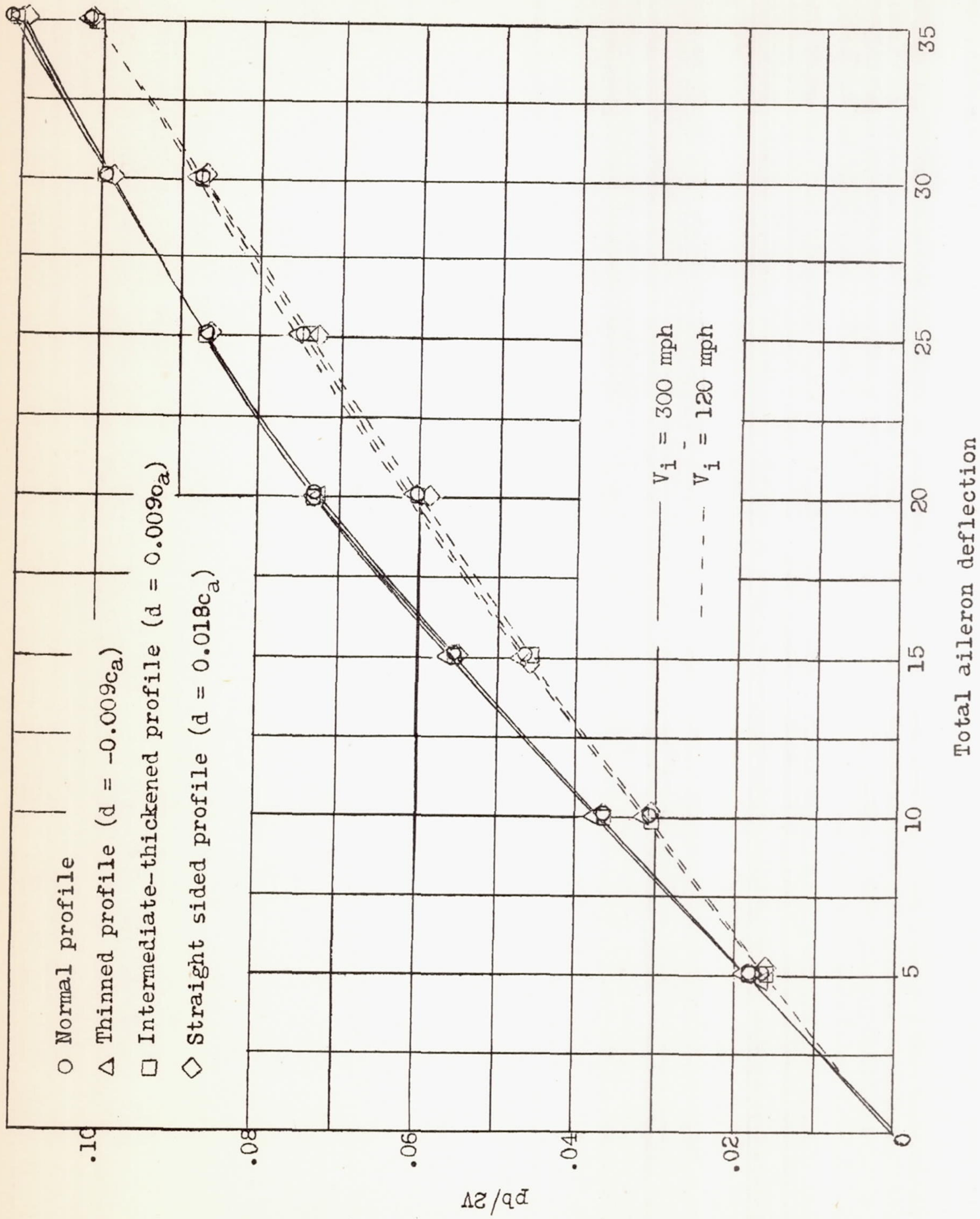

Figure 21.- The influence of profile on aileron effectiveness as applied to a typical pursuit airplane, 0.20-chord, sealed gap ailerons; equal up and down aileron deflection; assumed rigid wing and zero sideslip.

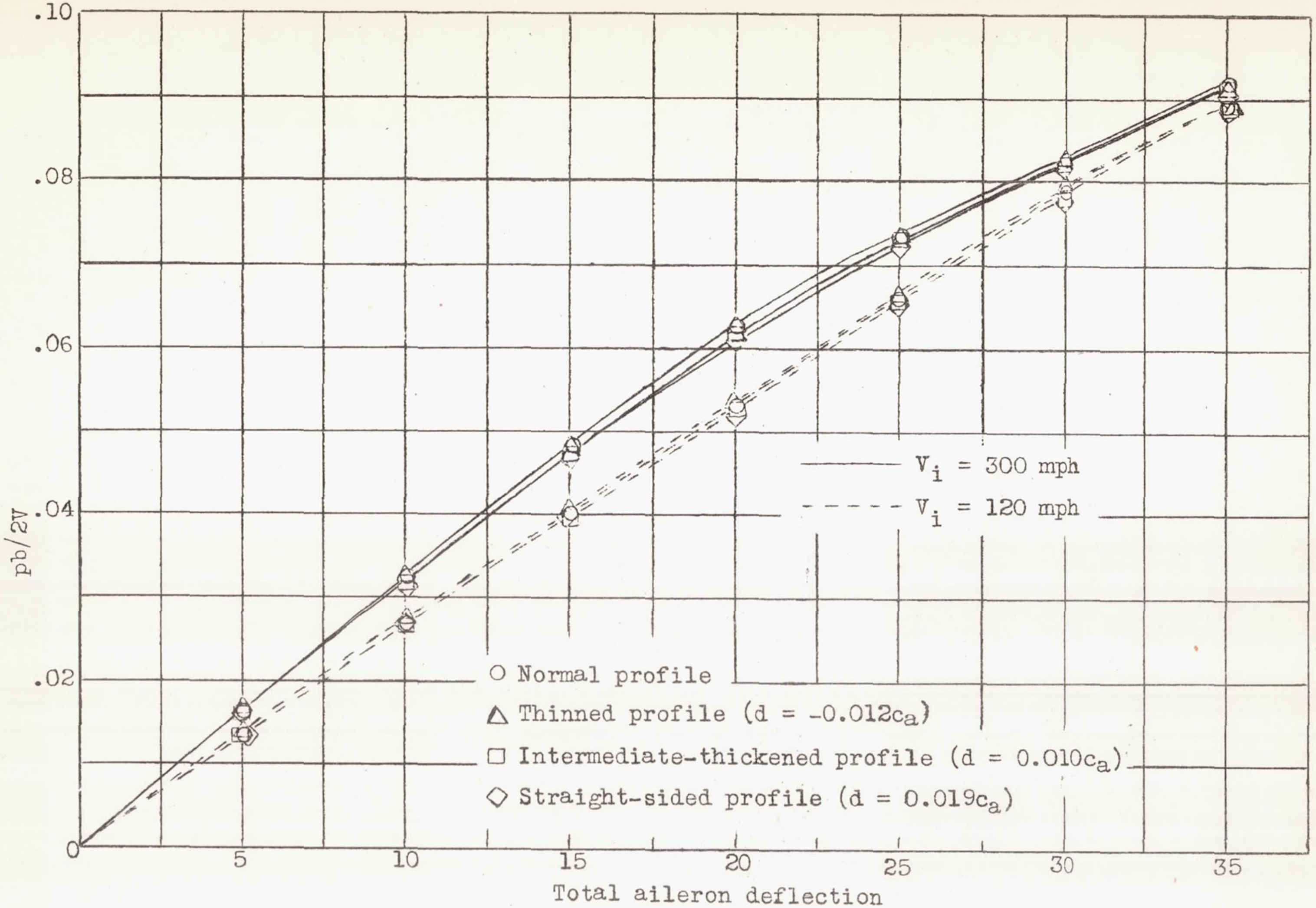

Figure 22.- The influence of profile on aileron effectiveness as applied to a typical pursuit airplane. 0.15-chord, sealed gap ailerons; equal up and down aileron deflection; assumed rigid wing and zero sideslip.

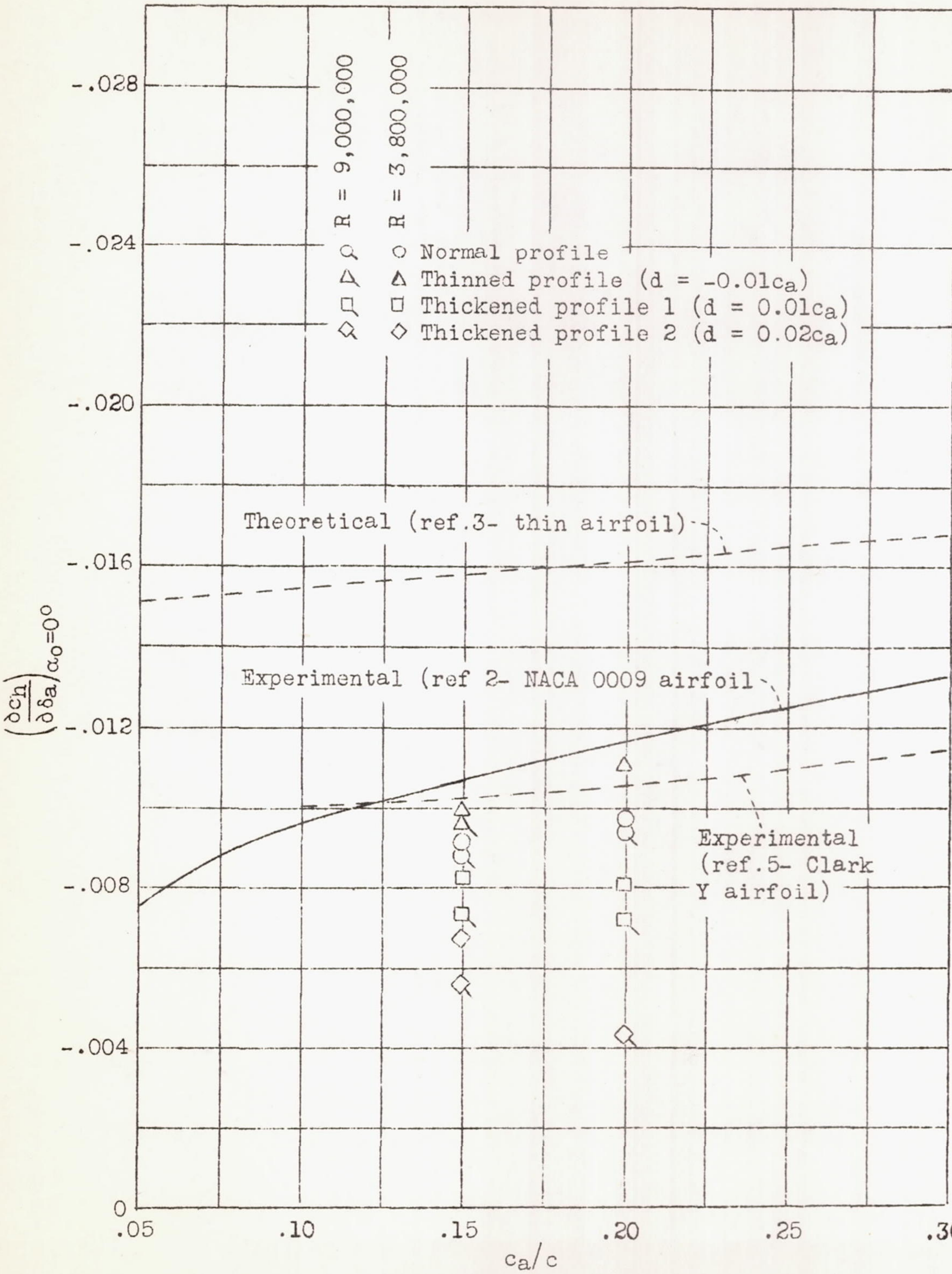

Figure 23.- The effect of modifications of the aileron profile on $(\partial c_h/\partial \delta_a)_{\alpha_0=0^\circ}$ for sealed gap, plain ailerons on an NACA 66,2-216 (a=0.6) airfoil.

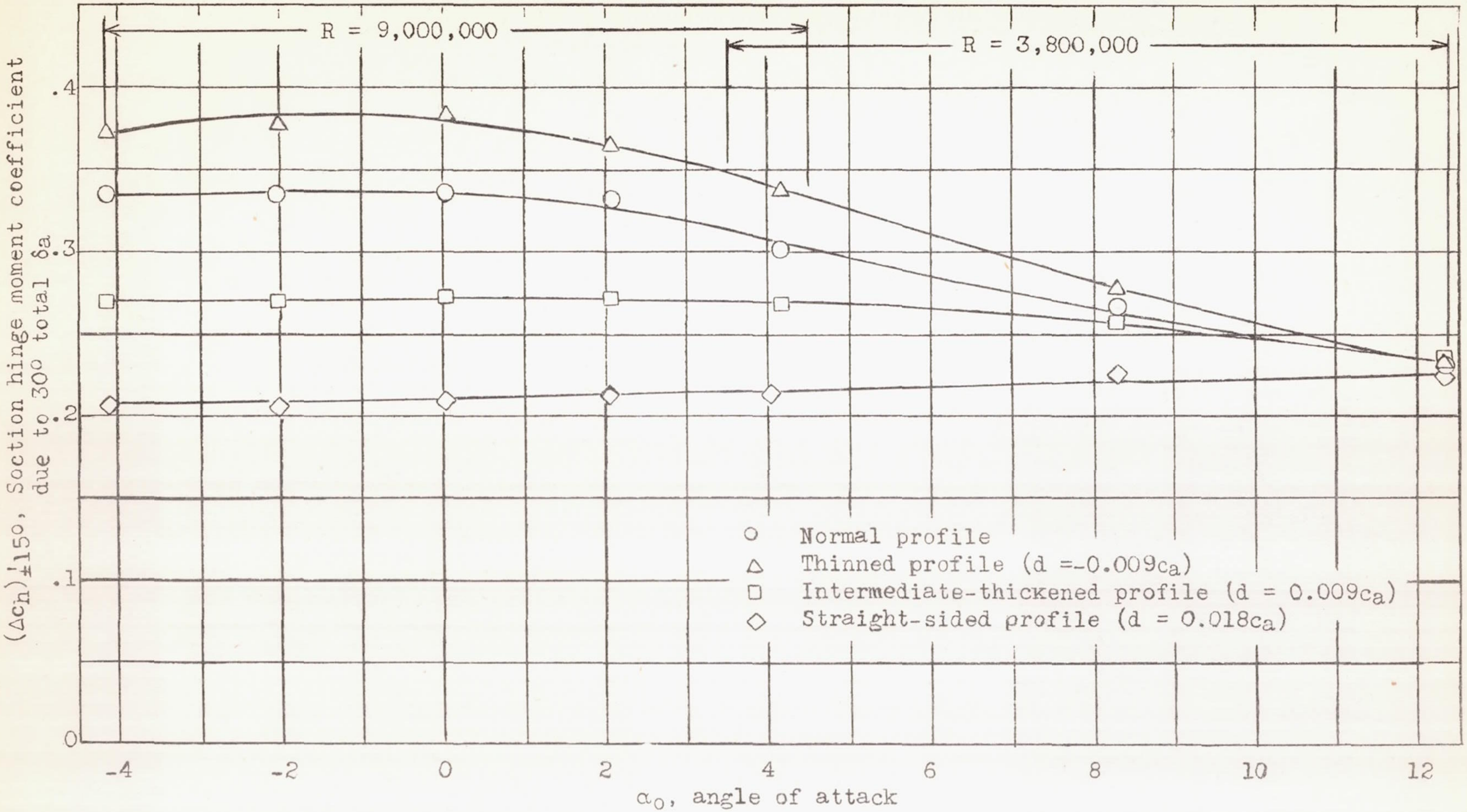

Figure 24.- The effect of modifications of the aileron profile on the total section hinge moment coefficient due to ±15° of aileron deflection for 0.20-chord, sealed gap, plain ailerons on an NACA 66,2-216 (a=0.6) airfoil.

A-55

NACA

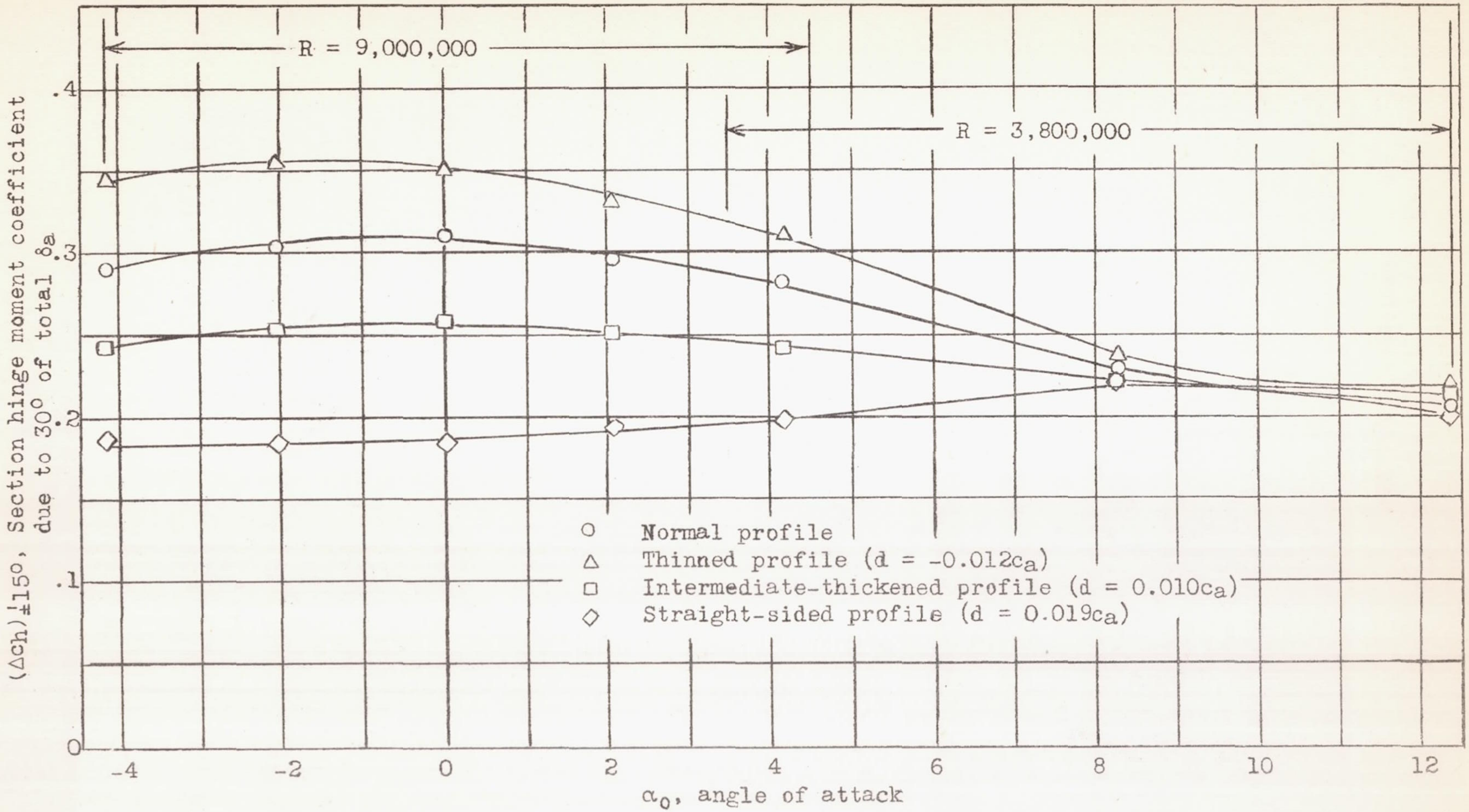

Figure 25.- The effect of modifications of the aileron profile on the total section hinge moment coefficient due to ±15° of aileron deflection for 0.15-chord, sealed gap, plain ailerons on an NACA 66,2-216 (a=0.6) airfoil.

Fig. 25

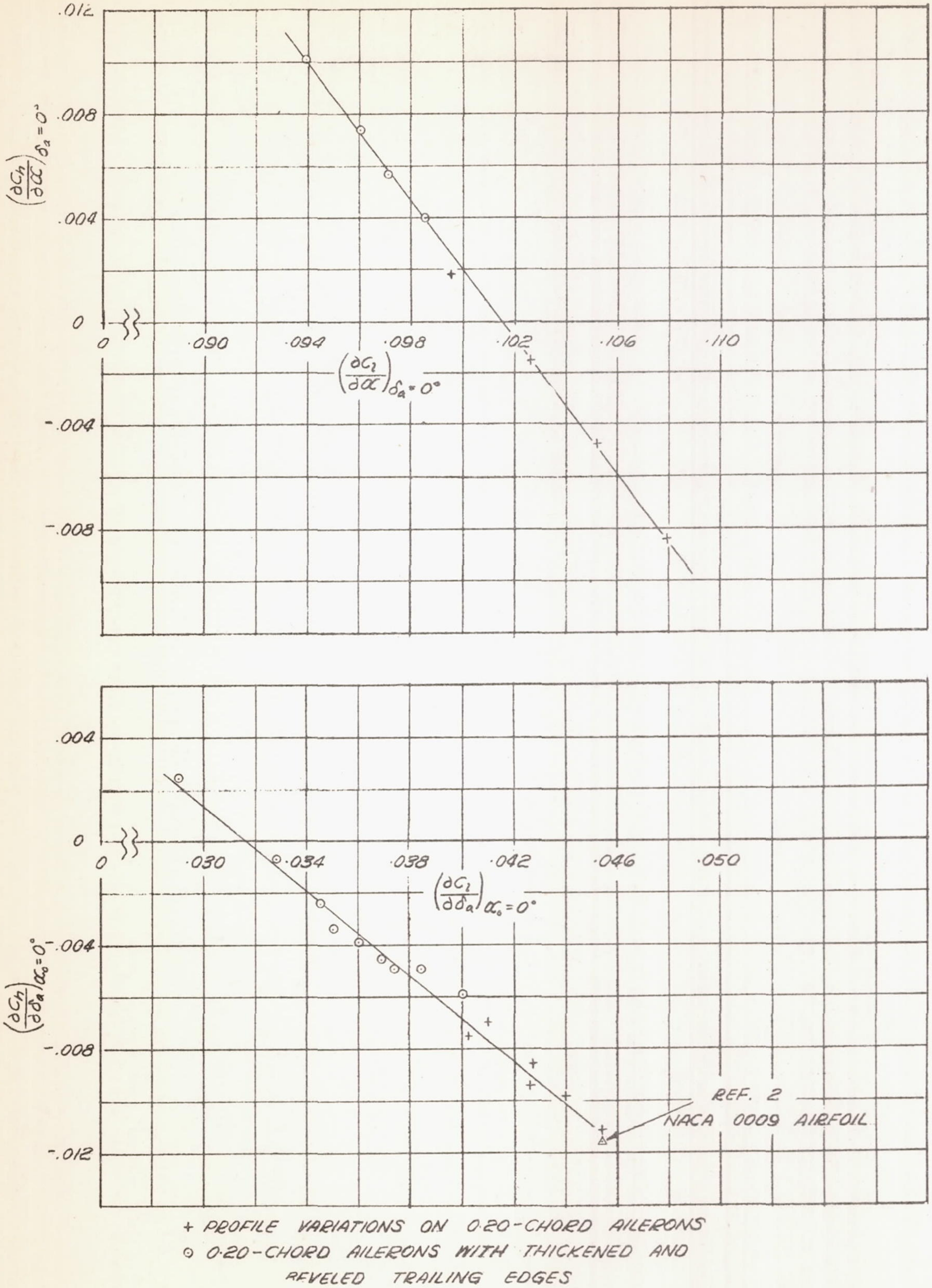

(1 block = 10/30")

FIGURE 26.- THE VARIATION OF HINGE MOMENT PARAMETERS WITH LIFT PARAMETERS FOR AN NACA 66,2-216 (a=0.6) AIRFOIL EQUIPPED WITH A 0.20-CHORD, SEALED GAP, PLAIN AILERON

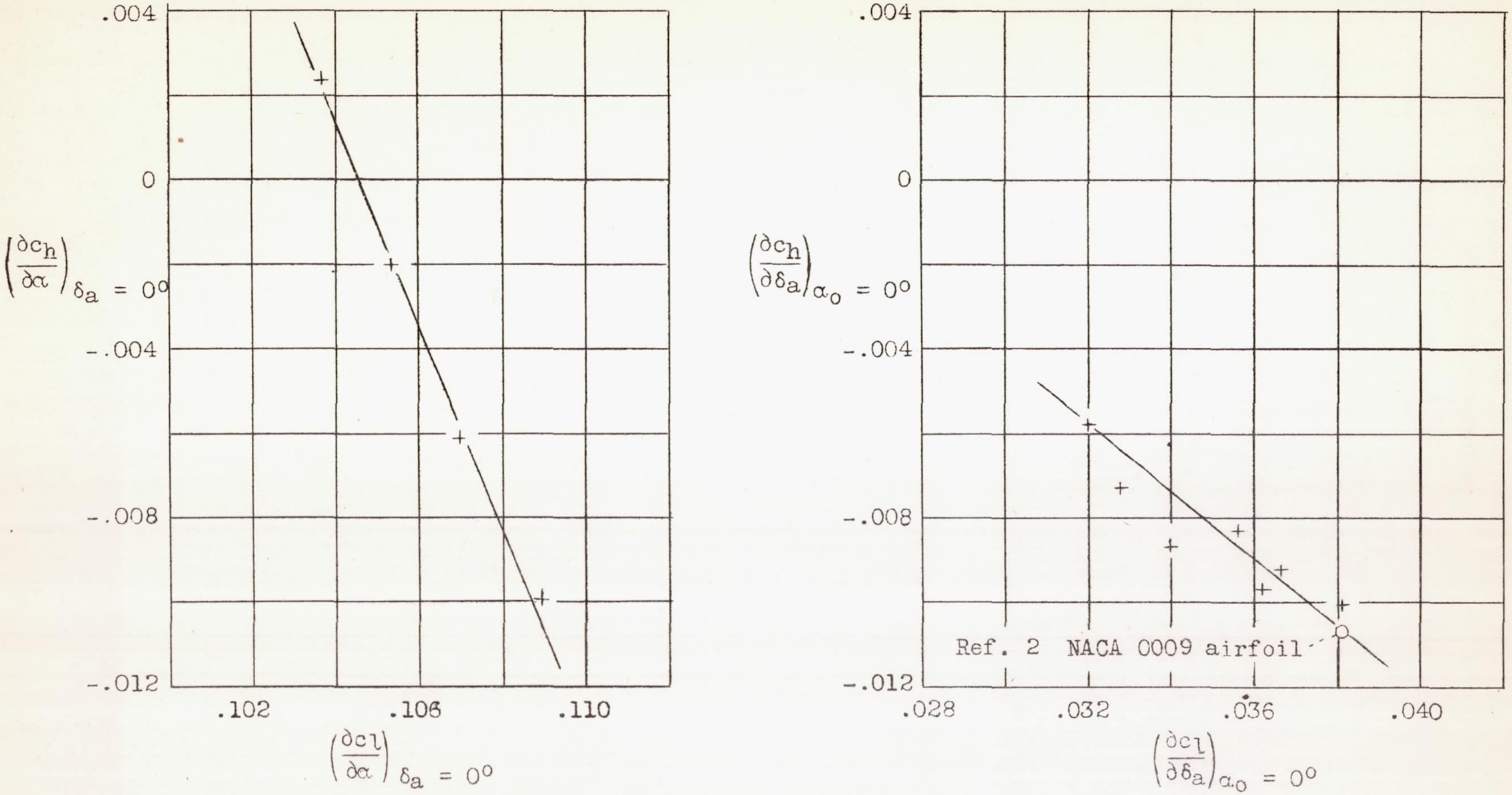

Figure 27.- The variation of hinge moment parameters with lift parameters for an NACA 66,2-216 (a=0.6) airfoil equipped with a 0.15-chord, sealed gap, plain aileron.

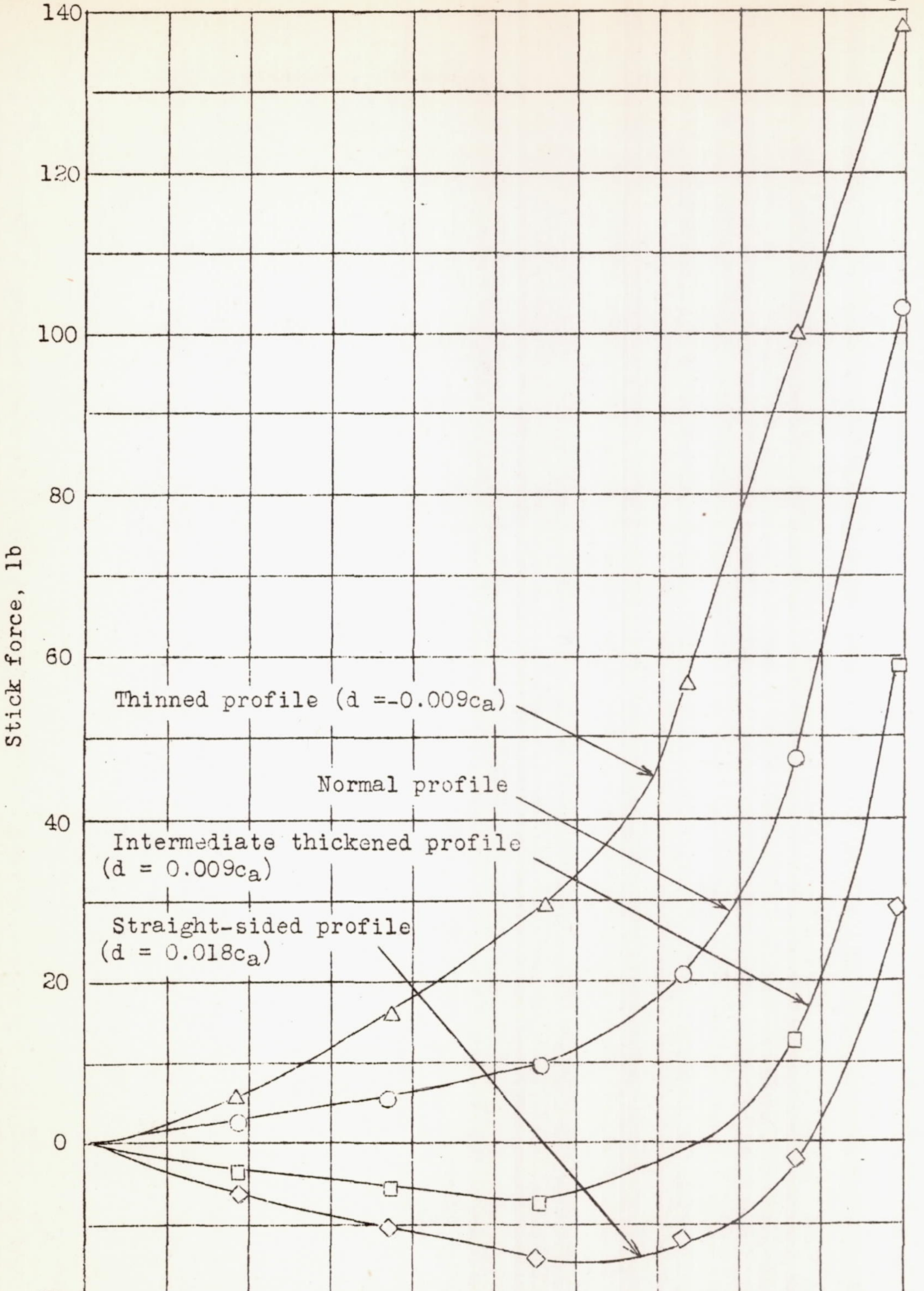

Figure 28.- The effect of modifications of the aileron profile on the aileron-control characteristics of a typical pursuit airplane equipped with 0.20-chord, sealed gap ailerons with $0.53c_a$ internal nose balance at an indicated airspeed of 300 mph.

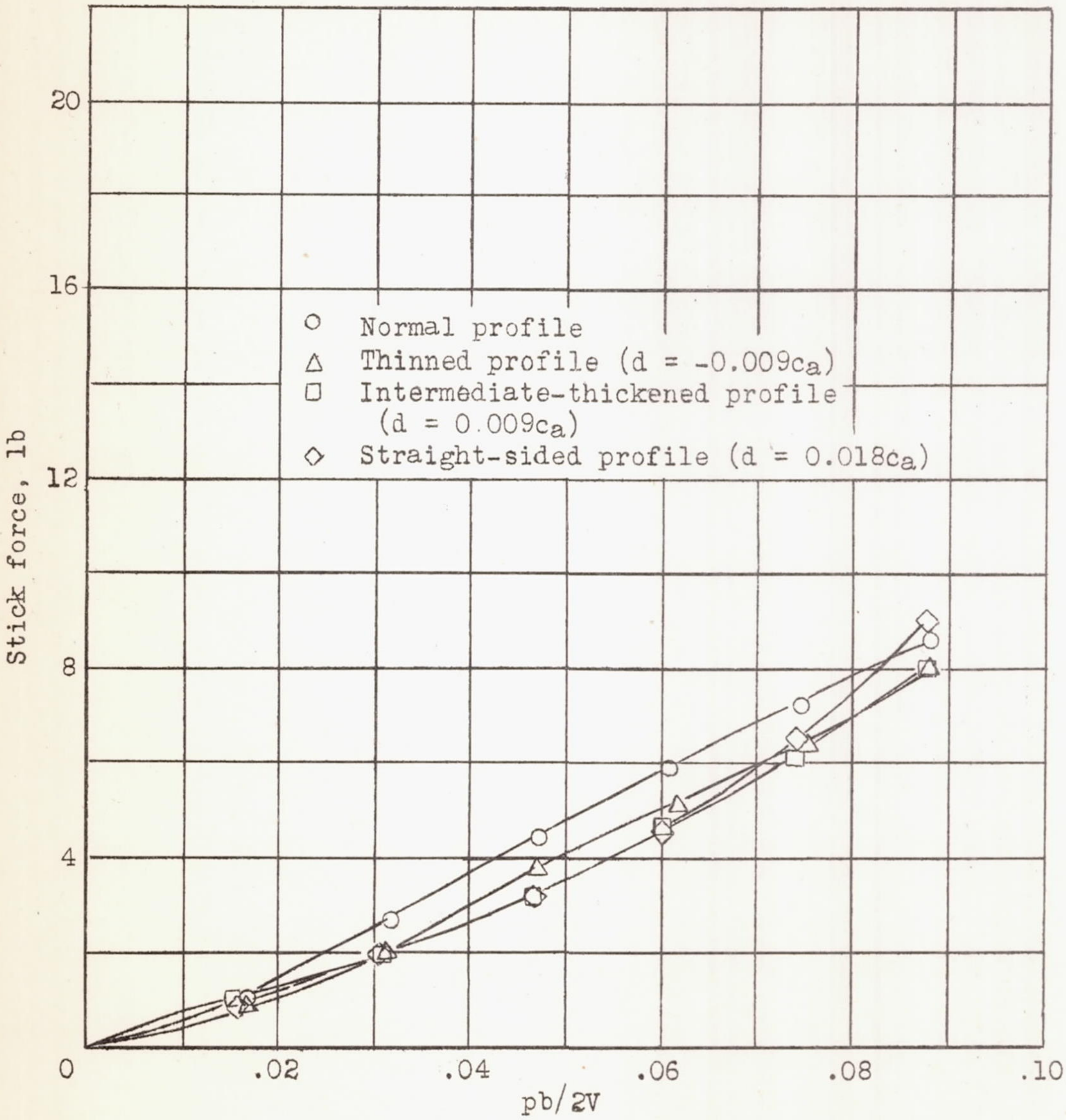

Figure 29.- The effect of modifications of the aileron profile on the aileron-control characteristics of a typical pursuit airplane equipped with 0.20-chord, sealed gap ailerons with $0.53c_a$ internal nose balance at an indicated airspeed of 120 mph.

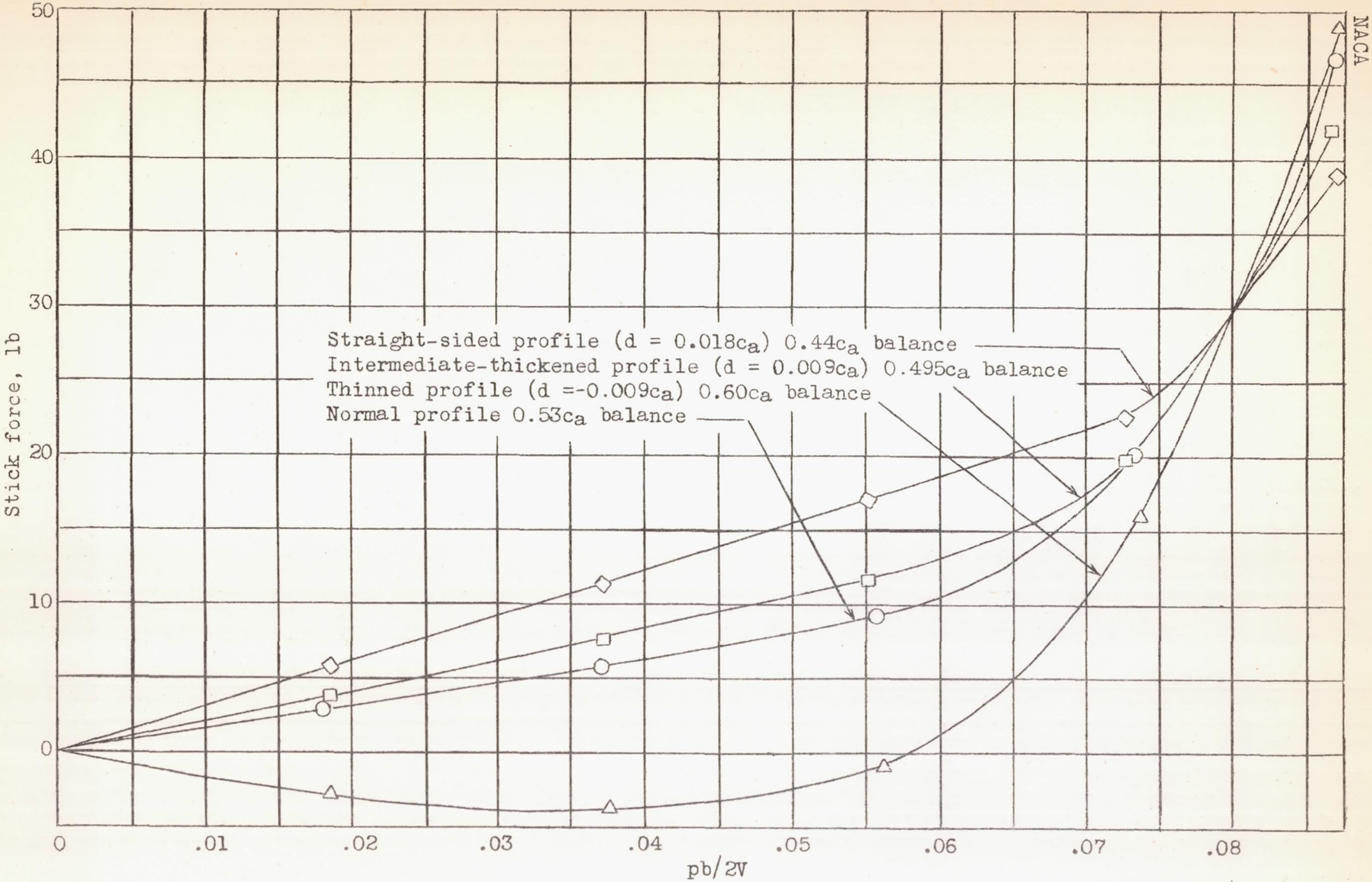

Figure 30.- The effect of modifications of the aileron profile on the aileron-control characteristics of a typical pursuit airplane equipped with 0.20-chord, sealed gap ailerons with sufficient internal nose balance for a 30-pound, high-speed, stick force at a pb/2V of 0.08. V_i = 300 mph.

Fig. 30

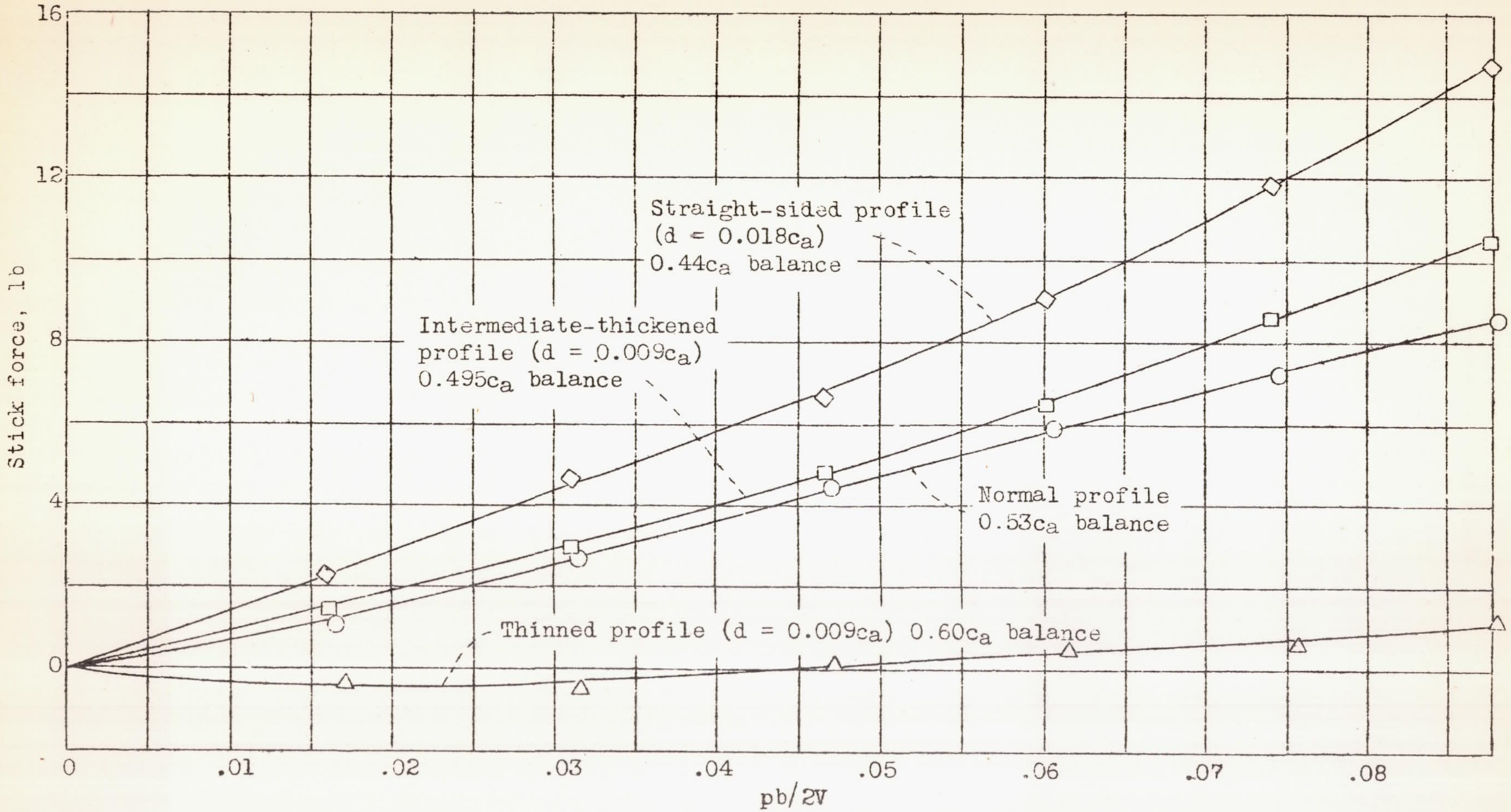

Figure 31.- The effect of modifications of the aileron profile on the aileron-control characteristics of a typical pursuit airplane equipped with 0.20-chord, sealed gap ailerons with sufficient internal nose balance for a 30-pound, high speed, stick force at a pb/2V of 0.08. V_i = 120 mph.

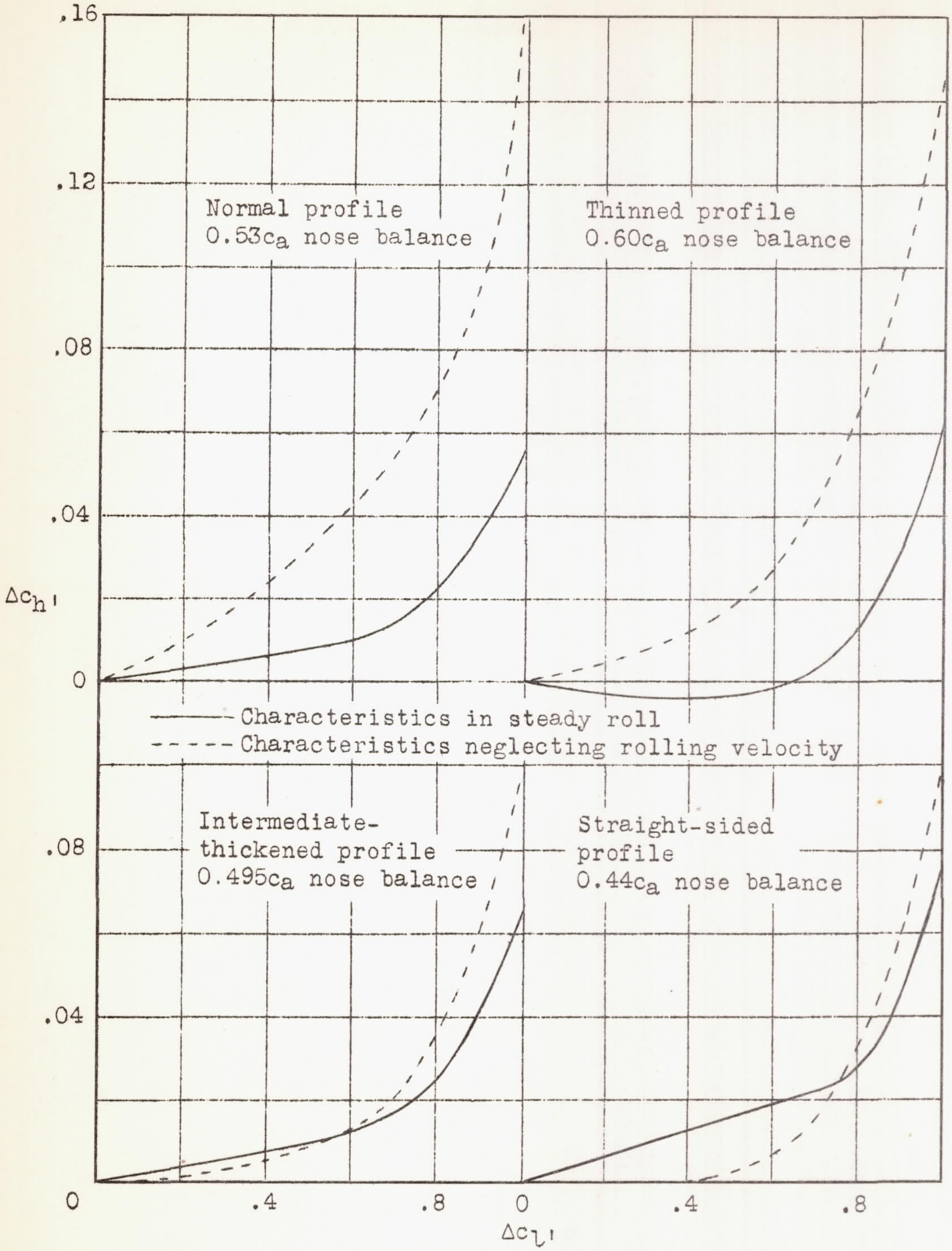

Figure 32.- The variation of total hinge moment coefficient with section lift coefficient increment for various 0.20-chord aileron profiles, showing the effect of aileron profile on the response factor (variation of c_h due to rolling). α_o=0.01°.

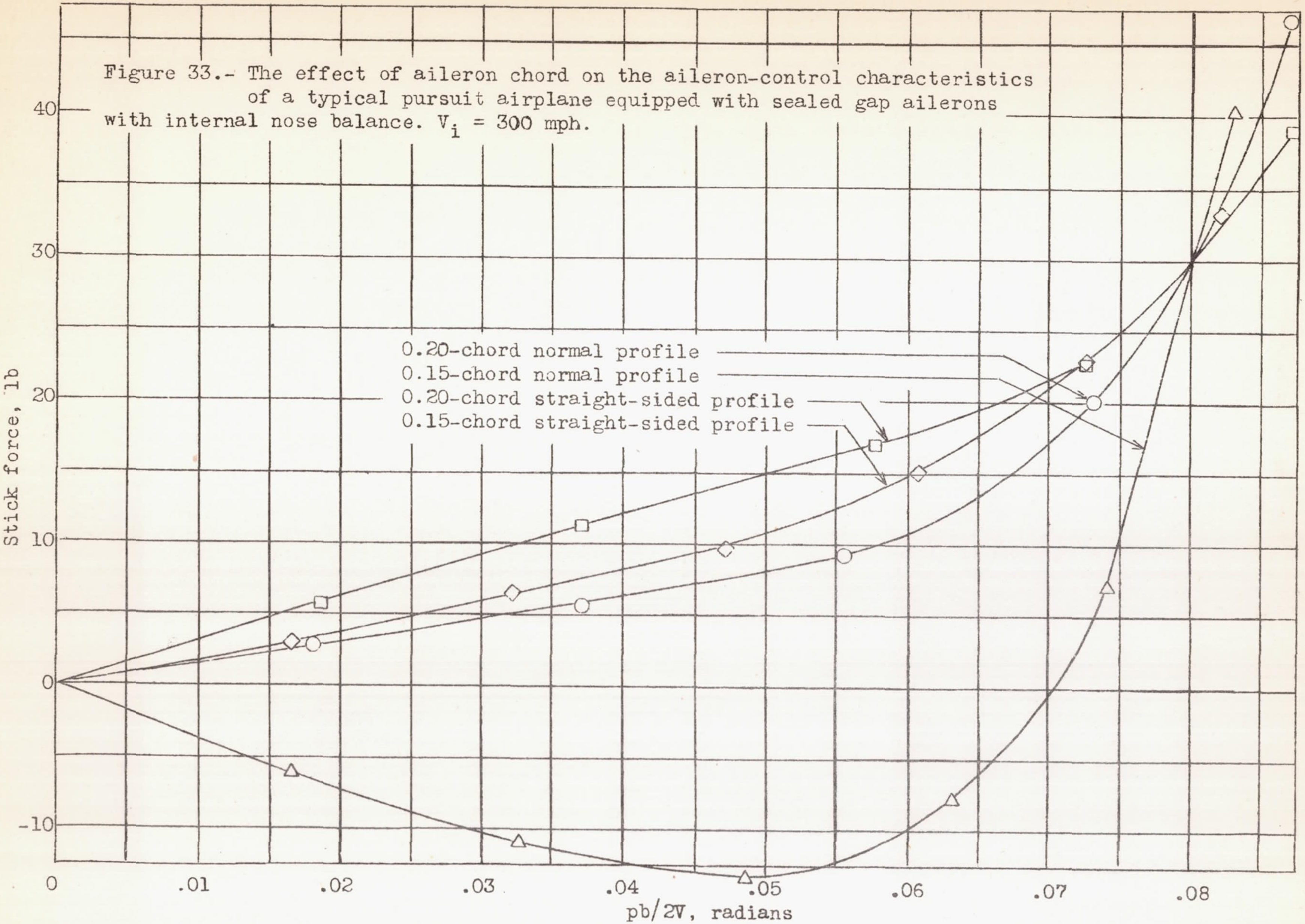

Figure 33.- The effect of aileron chord on the aileron-control characteristics of a typical pursuit airplane equipped with sealed gap ailerons with internal nose balance. V_i = 300 mph.

NACA

Fig. 33

(1 block = 10/40')

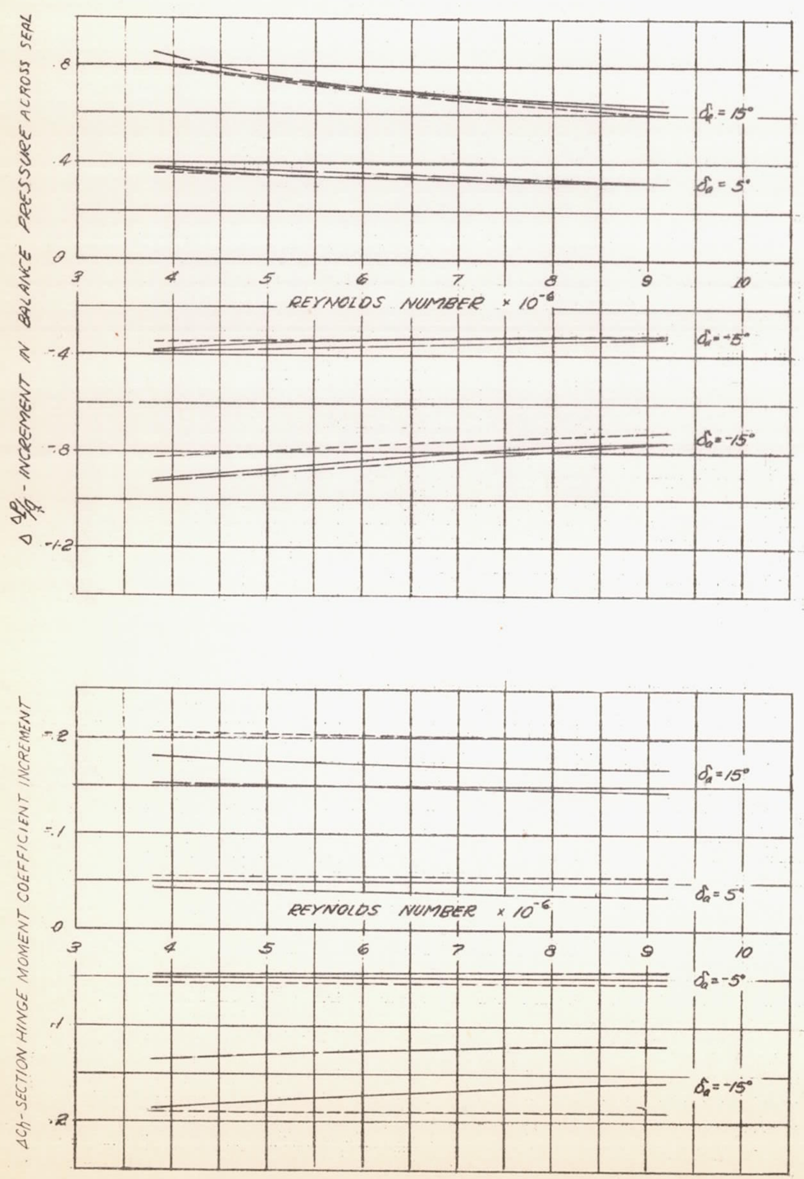

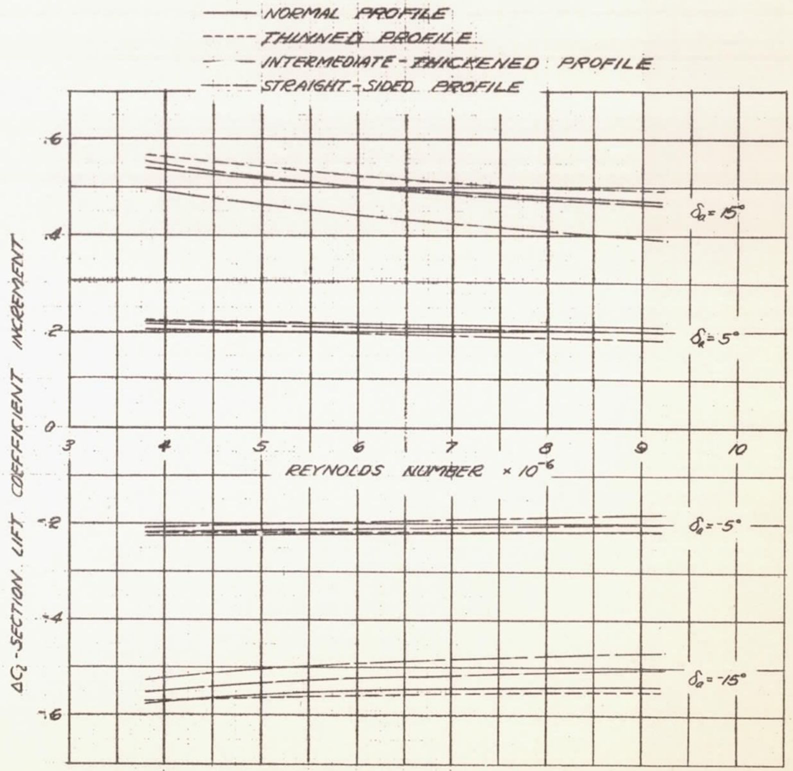

FIGURE 34.- THE EFFECT OF REYNOLDS NUMBER ON THE SECTION AERODYNAMIC CHARACTERISTICS OF AN NACA 66, 2-216 (a = 0.6) AIRFOIL EQUIPPED WITH 0.20-CHORD, SEALED GAP, PLAIN AILERONS. $\alpha_0 = 0.01°$

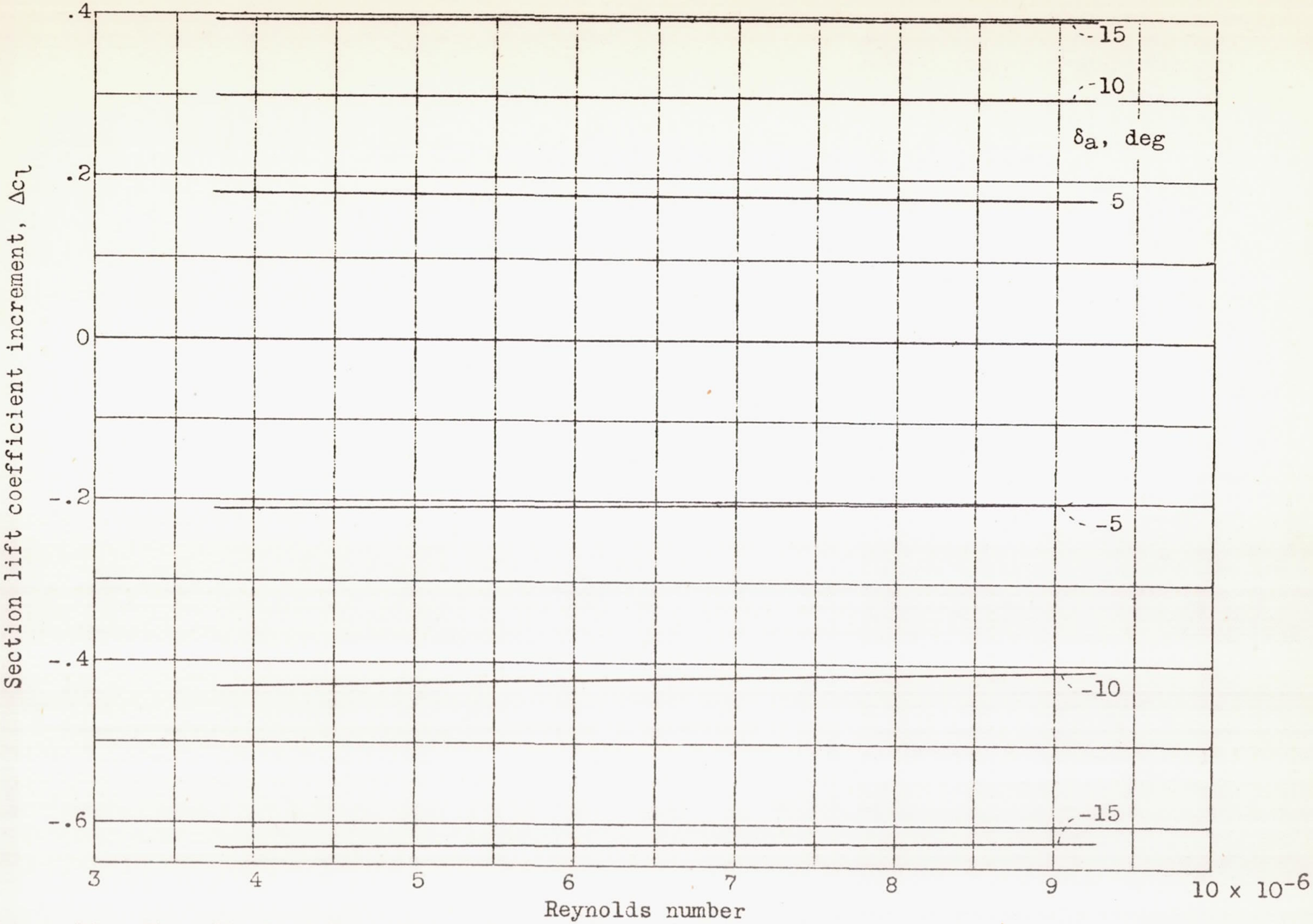

Figure 35.- The effect of Reynolds number on the section aerodynamic characteristics of an NACA 66,2-216 (a=0.6) airfoil equipped with 0.20-chord, sealed gap, plain ailerons of normal profile. $\alpha_o = 4.14^o$.

Fig. 36

(1 block = 10/40")

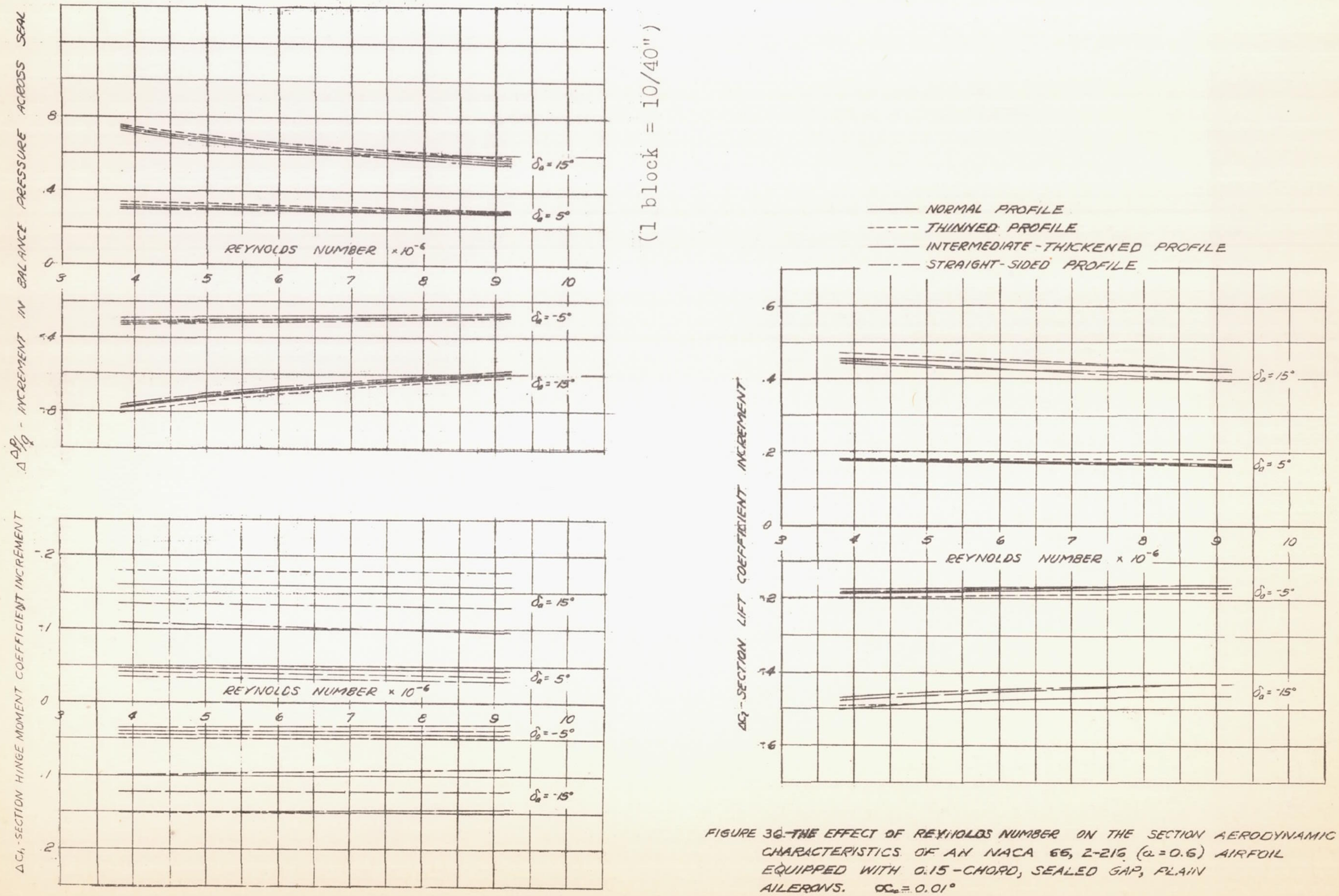

FIGURE 36.- THE EFFECT OF REYNOLDS NUMBER ON THE SECTION AERODYNAMIC CHARACTERISTICS OF AN NACA 66, 2-216 ($a = 0.6$) AIRFOIL EQUIPPED WITH 0.15-CHORD, SEALED GAP, PLAIN AILERONS. $\alpha_o = 0.01°$

NACA